Thesis for the Degree of Master of Engineering

Flow and heat transfer characteristics of the Master Joint in a floor heating system

by

Tran Manh Vu

Department of Mechanical Engineering

The Graduate School

Pukyong National University

February 2007

Flow and heat transfer characteristics of the Master Joint in a floor heating system

(바닥 난방시스템의 마스터 열유동특성)

Advisor : Prof. Oh Boong Kwon

by

Tran Manh Vu

A thesis submitted in partial fulfillment of the requirements
for the degree of

Master of Engineering

in Department of Mechanical Engineering
The Graduate School
Pukyong National University

February 2007

Tran Manh Vu 의 공학석사 학위논문을

인준함

2006 년 12 월 26 일

주 심 공학박사 김 민 남 (인)

위 원 공학박사 배 대 석 (인)

위 원 공학박사 권 오 봉 (인)

Flow and heat transfer characteristics of the Master Joint in a floor heating system

A dissertation

by

Tran Manh Vu

Approved by:

(Chairman) **Prof. MIN NAM KIM**

(Member) **Prof. DAE SEOK BAE**

(Member) **Prof. OH BOONG KWON**

February 28, 2007

바닥 난방시스템의 마스터 열유동특성

Tran Manh Vu

부 경 대 학 교 대 학 원

기 계 공 학 과

요 약

한국의 전통 난방 방식인 온돌난방에서, 바닥의 난방 및 배관 방식에 대한 여러 연구가 진행되어 왔다. 본 논문은 히트 파이프나 열사이폰을 이용한 난방방식 을 다루며, 이 난방 시스템의 중요한 부분은 온수관의 온수로부터 히트 파이프 또는 열사이폰으로 열을 전달하는 부위인 마스터 조인트 부분이며, 이 부분에서의 유동 및 열전달 특성에 관하여 논의한다. 기존의 마스터 조인트에 대한 수치 시뮬레이션을 행하여 유동 및 열전달 특성을 파악하고 단점을 개선하여 새로운 마스터 조인트를 제안하였으며, 새 마스터 조인트에 대한 수치 시뮬레이션을 행하여 기존의 마스터 조인트와 유동 및 열전달 특성을 비교하였다.

Flow and heat transfer characteristics of the Master Joint in a floor heating system

Tran Manh Vu

Department of Mechanical Engineering
The Graduate School
Pukyong National University

Abstract

A traditional Korean heating system in residential homes is a floor heating system, “ondol”. With the development of society, many kinds of floor heating systems were investigated to increase heat transfer to the floor. In this study, a new floor heating system using heat pipes or thermal siphons is discussed. It consists of main pipes where hot water flows, heat pipes or thermal siphons, and master joints where thermal energy of hot water is transferred to the heat pipes or thermal siphons.

In this new floor heating system, one of the most important parts is the master joint. Its shape plays an important role in heat transfer of this system. At first, numerical simulations were carried out to see the flow patterns, temperature distributions of the conventional existing master joint. Then, a new master joint which increases the performance of heat transfer of the floor heating system is proposed. To see the improvement of the new master joint, flow patterns, temperature distributions of two master joint models are compared. Also, in this study, flow characteristics and temperature distributions for several main hot water pipe diameters are shown and discussed to see the effects of main pipe diameter on this floor heating system.

ACKNOWLEDGEMENTS

The help and continuous support from professors, colleagues, friends, and family to whom I am most grateful, will never be forgotten. Without you, all of you, I would not be what I am today. I would like to thank each of you individually by word, but I do so in my heart.

At first, I would like to express my deepest gratitude to my supervisor, Professor Oh Boong Kwon (권오붕 교수님), with a spirit of enterprise for his strong support and patient guidance, encouragement and advice in this study. I appreciate the time spent with him in the numerous discussions in this research. His rich knowledge and practical experience in the thermo fluid engineering has been also most helpful in guiding this study. Our discussions and his suggestion with regards to fluid mechanics and heat transfer have been of great value. I have learned a lot from his thorough and insightful review of this research and his dedication to producing high quality and practical research. Financial supports from the Professor during Master studying period are also gratefully acknowledged.

I would like to recognize the contributions and helpful suggestions provided by my thesis advisory committee members Professor Min Nam Kim (김민남 교수님) and Professor Dae Seok Bae (배대석 교수님). These two Professors have given me their valuable comments, feedback and great suggestions based on their work, thus greatly contributing to the improvement, refinement and final completion of my thesis..

Sincere gratitude is extended to Professors of the Department of Mechanical Engineering in Pukyong National University and the Faculty of Civil Engineering in HoChiMinh City University of Technology, who

provided many engineering tools and knowledge background that I have gained from their classes.

I show great appreciation to members of Thermo Fluid Engineering Lab. for giving me a comfortable and active environment as well as enthusiastic and invaluable help during the periods of time spent working with them. They all, in this way or another, have helped me a lot from the time of my first step here to the time of my graduation. Also, thanks are sent to Vietnamese students who have studied in Pukyong National University and Korea Maritime University, for their abroad friendly atmosphere and their encouragement.

Finally, and perhaps most importantly, I wish to express my sincere appreciation to my parents, who have brought up and taught me how to live. And thanks to my sisters and my girl friend for their companionship, endless love, endurance, and continuous encouragement. Without all of you, this study would not have been possible.

Pukyong National University, Busan, Korea

December, 2006

Tran Manh Vu

TABLE OF CONTENTS

LIST OF TABLES

LIST OF FIGURES

NOMENCLATURE

SYMBOLS

C_p	:	Constant pressure specific heat	[J/kg·K]
d	:	Diameter of the main pipe	[m]
g	:	Gravitational acceleration	[m/s^2]
H	:	Actual head rise	[m]
k	:	Turbulent kinetic energy	[m^2/s^2]
$\dot{m}$	:	Mass flow rate	[kg/s]
P	:	Pump capacity	[W]
Q	:	Flow rate	[m^3/s]
$\dot{Q}$	:	Heat transfer rate	[J/s]
T	:	Temperature	[^oC or K]
x	:	x-coordinate	
y	:	y-coordinate	
z	:	z-coordinate	

GREEK SYMBOLS

γ	:	Specific weight	[N/m^3]
ε	:	Dissipation rate	[m^2/s^3]
ρ	:	Density	[kg/m^3]
Δp	:	Pressure difference	[Pa]
ΔT	:	Temperature difference	[K]

CHAPTER 1

INTRODUCTION

1.1 Background of study

Korea has four seasons and each season has distinctive features related to the climate. For the cool dry winter, the ondol heating system has been widely used as a residential heating system. Ondol is an excellent heating system because it efficiently uses both the radiative and convective heat transfer to achieve a high level of heating.

Nowadays, hot water radiant floor heating systems have been used instead of Korean traditional ondol systems to improve the thermal comfort, convenient maintenance and energy efficiency.

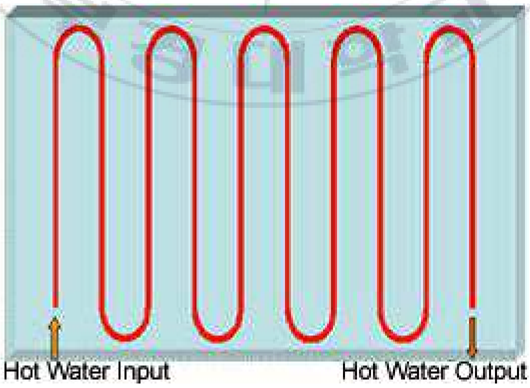

Fig. 1.1 Conventional floor heating system

Fig. 1.1 shows a conventional floor heating system used in Korea. As shown in this figure, hot water flowing in the pipes underneath is used to heat the floors of living rooms, bed rooms, etc.

These days in Korea, a new heating system using heat pipes or thermal siphons is widely used because of its heat transfer capacity. As shown in Fig. 1.2, it consists of main pipes where hot water flows, heat pipes or thermal siphons, and master joints where thermal energy of hot water is transferred to the heat pipes or thermal siphons.

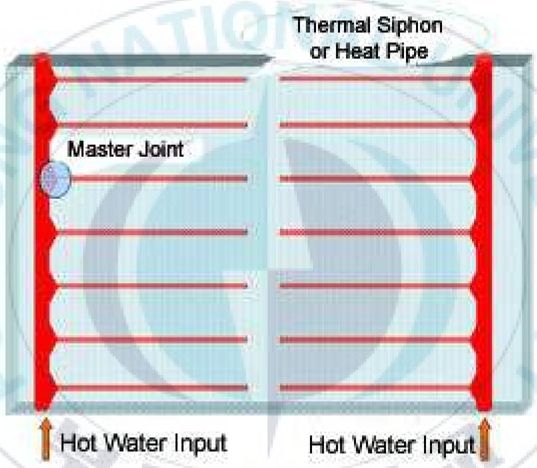

Fig. 1.2 New floor heating system with thermal siphons or heat pipes

In the new floor heating system, the shape of the master joint plays an important role in heat transfer of this system. It is necessary to improve the shape of the master joint for increasing heat transfer to the floor.

In this study, the present master joint is shown and discussed to see the restriction of heat transfer to the floor. Fig. 1.3 and Fig. 1.4 show the present master joint model used for the floor heating system.

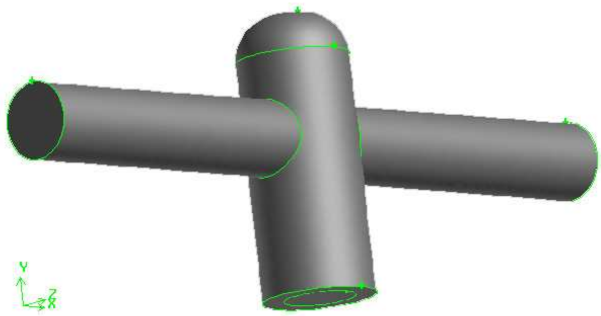

Fig. 1.3 Present master joint model

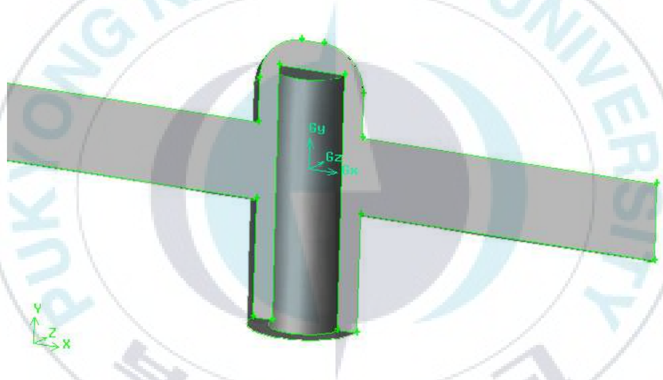

Fig. 1.4 Central vertical section of the present master joint model

To improve the heat transferred to the floor, a new master joint was proposed to increase the performance of heat transfer of the floor heating system. In this study, it will be compared with the present master joint using the flow pattern, velocity, temperature characteristic and heat transferred to the floor. A proposed master joint was shown in Fig. 1.5 and Fig. 1.6.

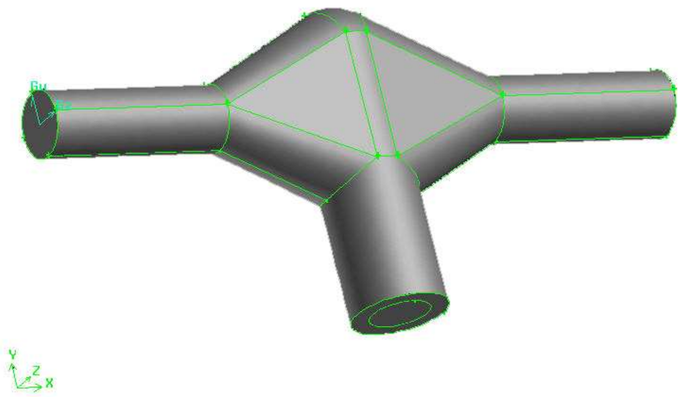

Fig. 1.5 New master joint model

Fig. 1.6 Central vertical section of the new master joint model

In order to increase the heat transferred to the floor, the effects of the main hot water pipe diameter will be determined. Flow characteristics and temperature distributions for four types of the main hot water pipe diameter are shown and discussed to see the effects of the main pipe diameter on this floor heating system.

1.2 Objectives and outline of the study

The purpose of this study is to find a new master joint for the floor heating system, to increase heat transfer to the floor. If the master joint is designed well, lots of heat will be transferred to the floor, so heat will be conserved. People will feel more comfortable in winter seasons and save a great deal of money for heating their rooms.

As mentioned above, a new master joint is proposed in this study to increase the heat transferred to the floor of residential homes. This study includes 5 chapters and the respective summary is briefly mentioned below.

- Chapter 1 shows the background of the floor heating system used in Korea and the role of the master joint in transferring heat to the floor.

- In chapter 2, flow patterns, velocity vectors, temperature distributions, pressure distributions and heat transfer characteristics of the present master joint are presented and discussed.

- The effects of main hot water pipe diameter are discussed in chapter 3. The flow patterns, velocity vectors, temperature distributions and heat transfer characteristics of the four sizes of the main hot water pipe diameter are determined.

- In chapter 4, a new model of the master joint is shown. It is compared with the present master joint model using the flow patterns, velocities, temperature characteristics and heat transferred to the floor.

- Chapter 5 summarizes the previous chapters and shows the final conclusion.

CHAPTER 2

REVIEW OF THE MASTER JOINT IN THE FLOOR HEATING SYSTEM

2.1 Introduction to the present master joint model

As mentioned in the previous chapter, a floor heating system consists of main pipes where hot water flows, heat pipes or thermal siphons, and master joints where thermal energy of hot water is transferred to the heat pipes or thermal siphons. In the present master joint model of this study, the diameter of the main hot water pipe is 17.5mm, the diameter of the heat pipe or thermal siphon is 16mm, and other geometry dimensions are shown in Fig. 2.1.

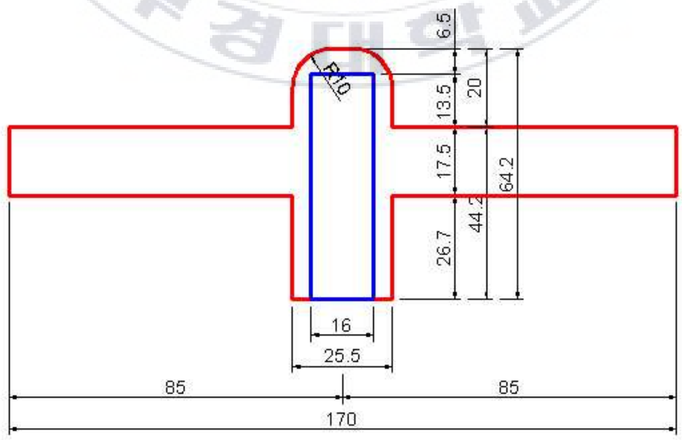

Fig. 2.1 Geometry dimensions of the present master joint model

GAMBIT was used for creating and meshing this model and FLUENT was used for solving the computations and distributing the results. Numerical simulations were carried out to see the flow patterns, temperature distributions and pressure distributions of this model.

In this study, a finite volume method was used for the discretization of the continuity equation, the momentum equations, and the energy equation. Hybrid scheme was used for the convection-diffusion terms and standard k-ε model was used as a turbulent model. Tetrahedral volume meshing scheme was used for meshing this model. The grids for the present master joint model used in the numerical simulations are shown in Fig. 2.2.

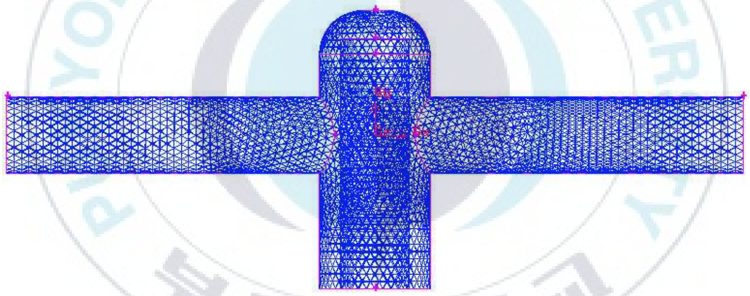

Fig. 2.2 Grids for numerical analysis of the present master joint model

For pressure boundary conditions, total gage pressure of 8000 Pa was given at the inlet of the main pipe and static atmospheric pressure was given at the outlet of the main pipe of the heating system. For temperature boundary conditions, 80^{o}C for hot water was used at the inlet of the main pipe, adiabatic conditions were used at walls of the master joint and isothermal conditions of 54^{o}C for the heat pipe or thermal siphon walls, were used in the numerical simulations.

2.2 Flow patterns and velocity vectors distributions

In order to see the flow patterns and velocity vectors distributions of the flow passing through the master joint, sections of this model were made. Fig. 2.3 shows velocity vectors at the central vertical section (z = 0) and Fig. 2.4 shows velocity vectors at the central horizontal section (y = 0) of the present master joint model. As clearly shown in these figures, velocities at upper and lower parts of the master joint are very small, while velocities at the center part of the master joint are relatively large. Therefore, hot water could not contact the entire surfaces of the heat pipe or thermal siphon.

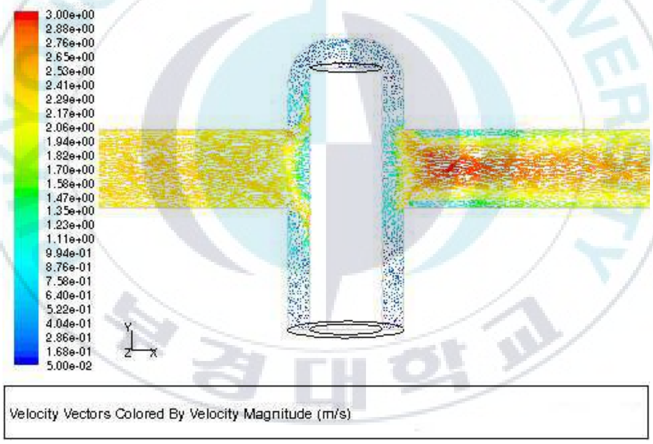

Fig. 2.3 Velocity vectors distribution at the central vertical section (z = 0)

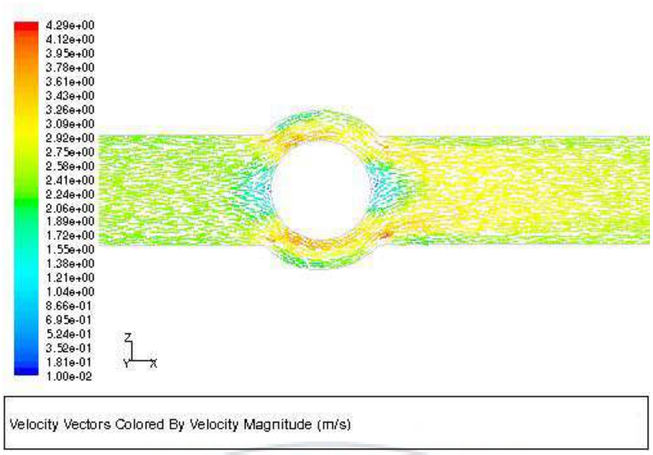

Fig. 2.4 Velocity vectors distribution at the central horizontal section (y = 0)

To see in more detail the velocities of the flow passing through the master joint, velocity vectors distributions at upper and lower parts were shown in larger scale in Fig. 2.5a and Fig. 2.6a. In Fig. 2.5b, velocity vectors at upper parts of the present model are shown in some horizontal sections, with y = 25mm, 20mm, 15mm, 10mm, 5mm, respectively. Similarly, Fig. 2.6b shows velocity vectors at lower parts of the present model in some horizontal sections, with y = –5mm, –10mm, –15mm, –20mm, –25mm, respectively.

In this present master joint model, separated flows occurred near the heat pipe or thermal siphon. These separated flows prevented the hot water passing through the master joint so the velocity of the flow was reduced. In order to a obtain higher velocity of the flow passing through the master joint, it is necessary to investigate other master joint models which can lower this disadvantage. This problem will be discussed in full in chapter 4.

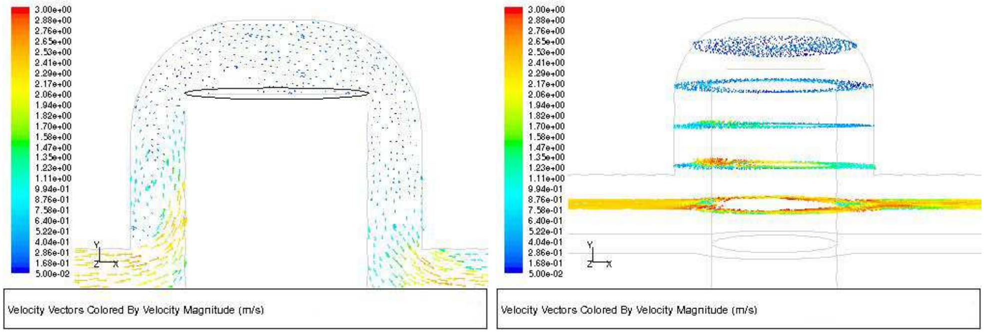

(a) (b)

Fig. 2.5a Velocity vectors distribution at upper part of the master joint model

Fig. 2.5b Velocity vectors distributions at some horizontal sections

(y = 25mm, 20mm, 15mm, 10mm, 5mm)

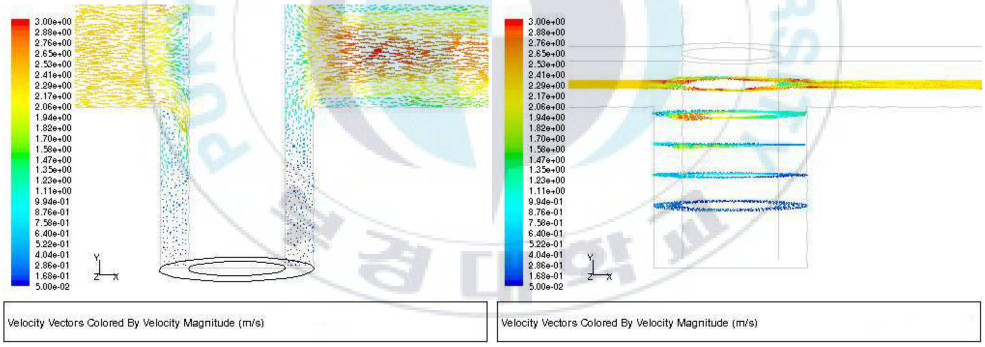

(a) (b)

Fig. 2.6a Velocity vectors distribution at lower part of the master joint model

Fig. 2.6b Velocity vectors distributions at some horizontal sections

(y = –5mm, –10mm, –15mm, –20mm, –25mm)

2.3 Temperature distributions

Temperature distribution is shown in Fig. 2.7a at the central vertical section (z = 0). In Fig. 2.7b, temperature distributions are shown in some horizontal sections with 5mm intervals on the y axis of the present master joint model, when total gage pressure of 8000 Pa was given at the inlet of the main pipe of the floor heating system.

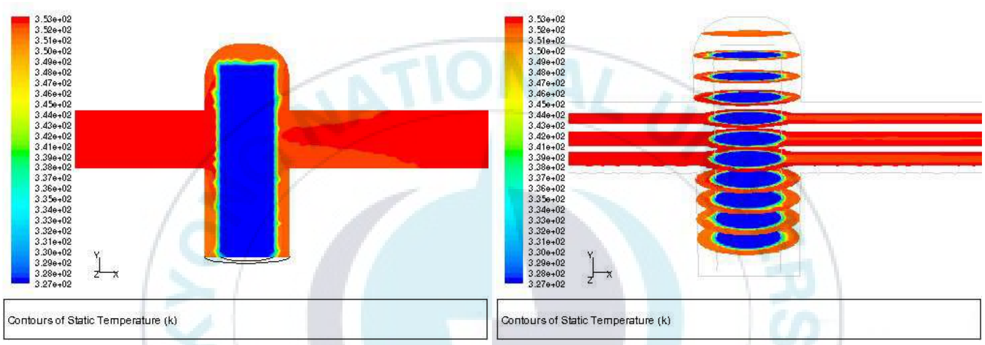

(a) (b)

Fig. 2.7a Temperature distribution at the central vertical section (z = 0)

Fig. 2.7b Temperature distributions at some horizontal sections (y = 25mm, 20mm, 15mm, 10mm, 5mm, 0, –5mm, –10mm, –15mm, –20mm, –25mm)

With temperature boundary conditions of 80^{o}C for the hot water used at the inlet of the main pipe, adiabatic conditions used in the walls of master joint and isothermal conditions of 54^{o}C used in the walls of heat pipe or thermal siphon, corresponding to the color scale, temperature fields at upper and lower parts of the master joint are relatively small, as shown in the above figures.

In this present model, the high temperature flow passed through the master joint and supplied thermal energy to the heat pipe or thermal siphon. Temperature of the flow going out the master joint toward the outlet reduced remarkably because hot water did not flow well at this area, as shown in Fig. 2.3 above. With this restriction, the heat pipe or thermal siphon in this model can not contract high temperatures, therefore the amount of heat transferred from hot water to the heat pipe or thermal siphon is rather small.

From Fig. 2.8 to Fig. 2.18, temperature fields in some horizontal sections with 5mm intervals on the *y* axis are shown. The left side figures show temperature distributions while the right side figures show the locations of these sections.

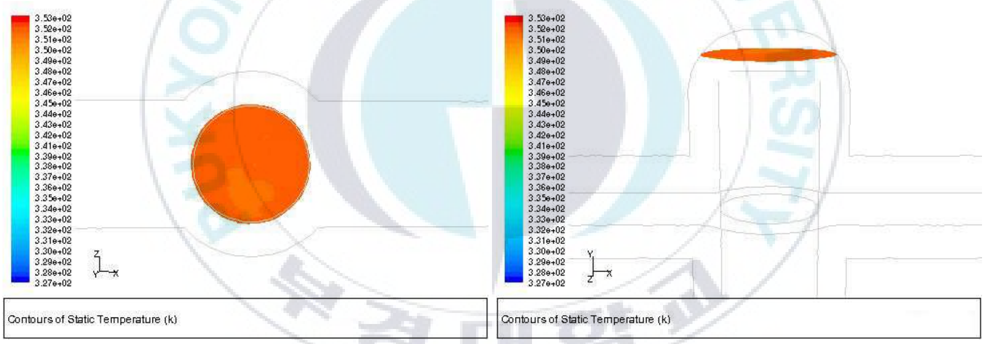

Fig. 2.8 Temperature distribution at section y = 25mm

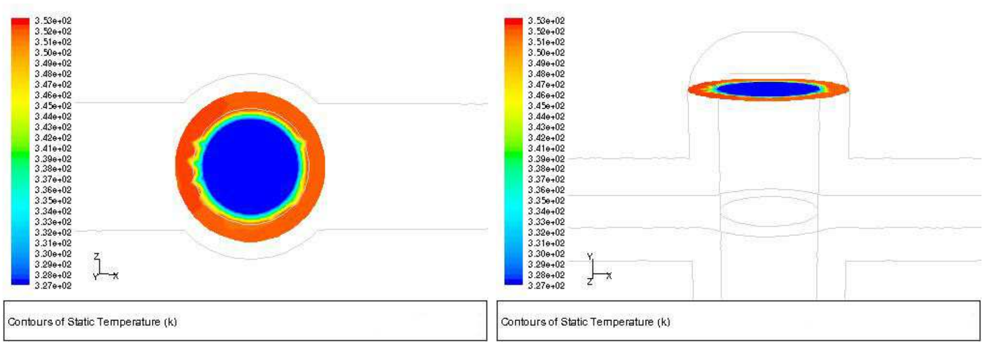

Fig. 2.9 Temperature distribution at section y = 20mm

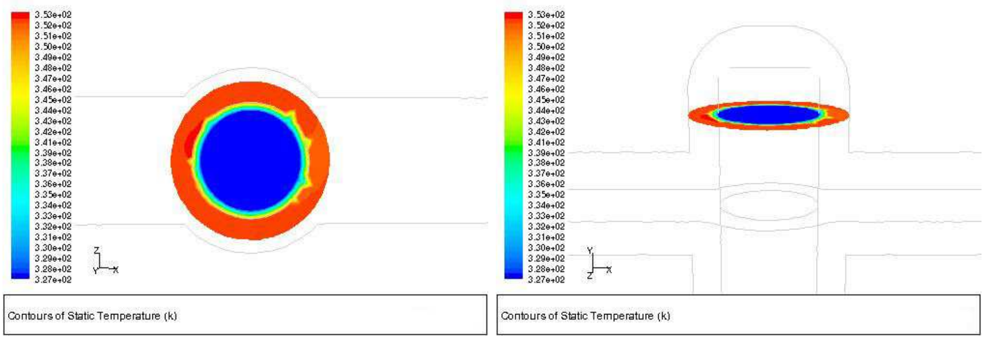

Fig. 2.10 Temperature distribution at section y = 15mm

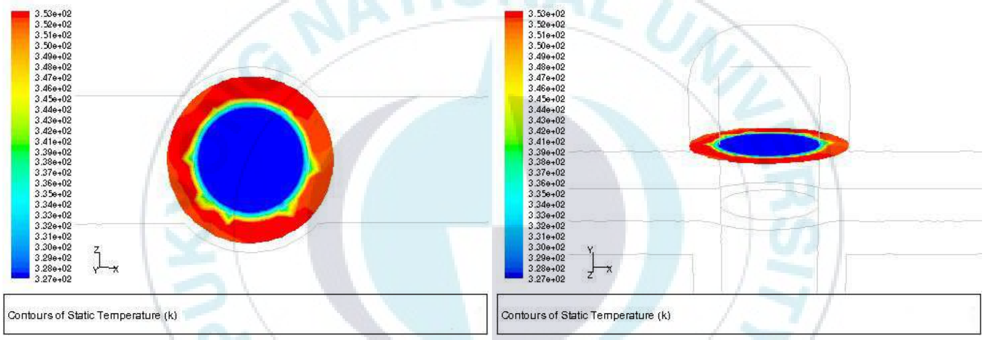

Fig. 2.11 Temperature distribution at section y = 10mm

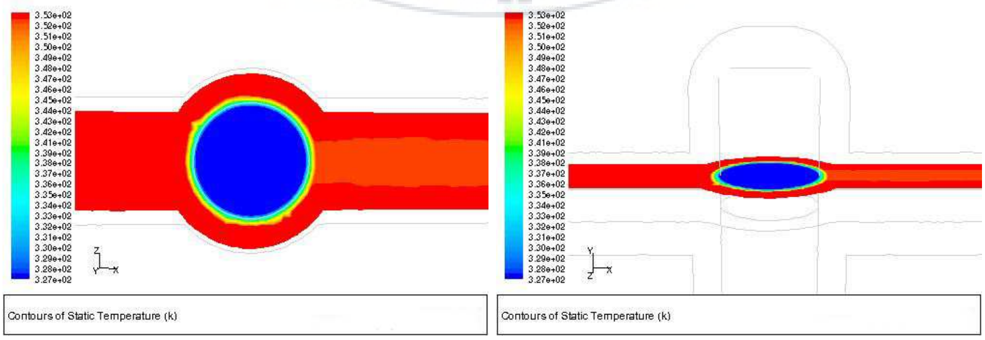

Fig. 2.12 Temperature distribution at section y = 5mm

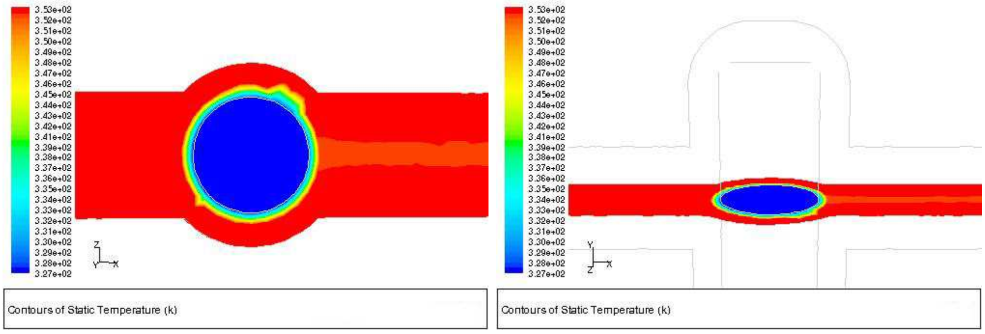

Fig. 2.13 Temperature distribution at section $y = 0$

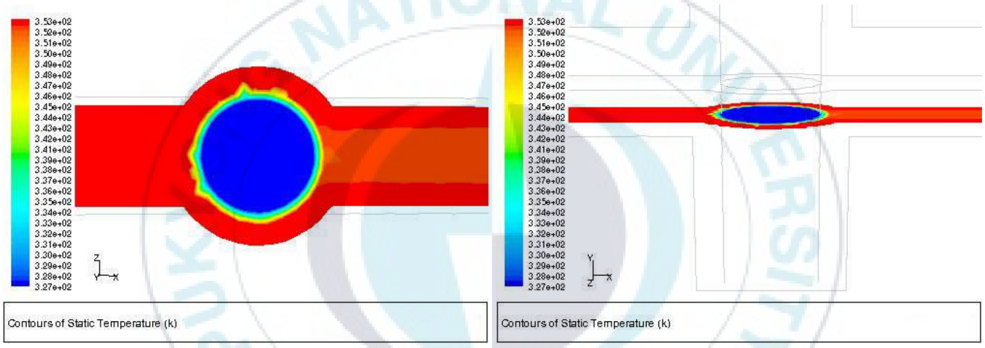

Fig. 2.14 Temperature distribution at section $y = -5$mm

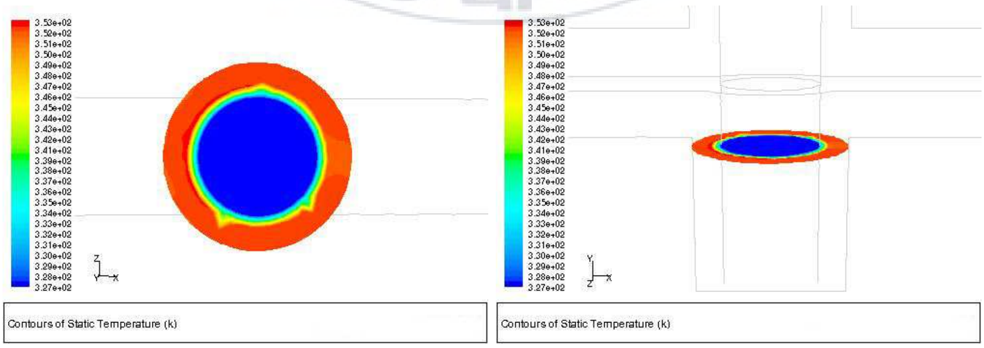

Fig. 2.15 Temperature distribution at section $y = -10$mm

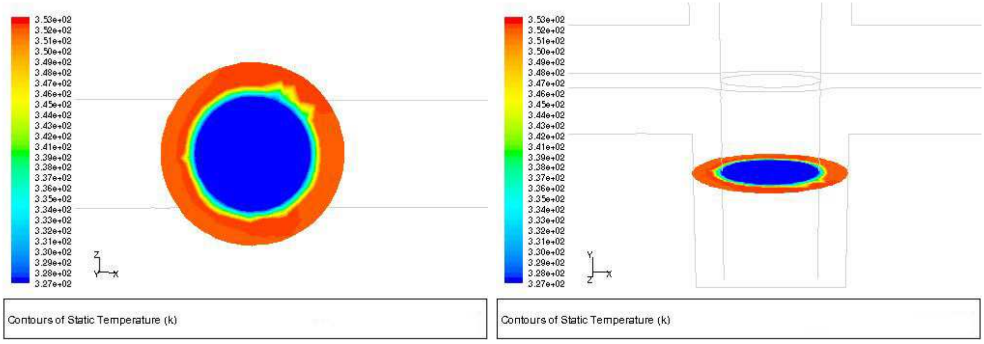

Fig. 2.16 Temperature distribution at section $y = -15$mm

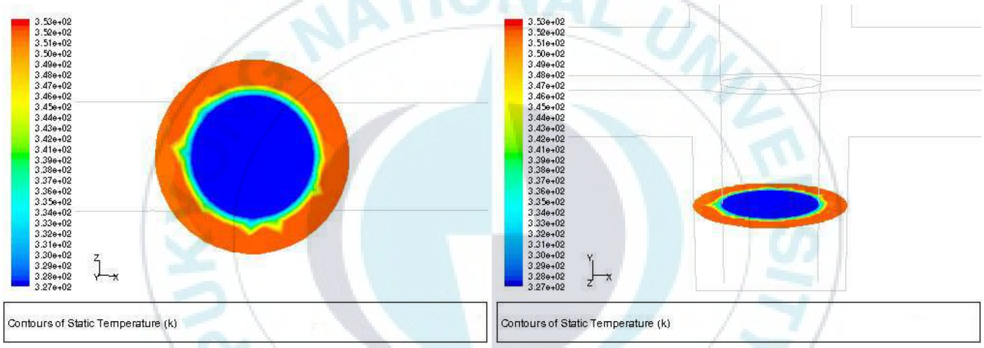

Fig. 2.17 Temperature distribution at section $y = -20$mm

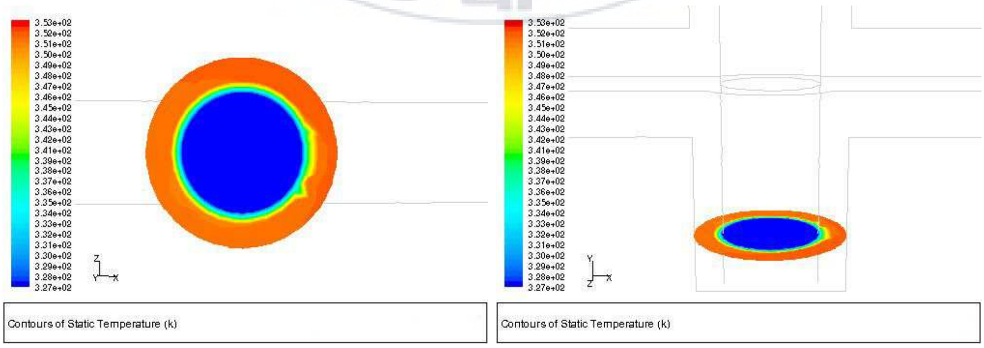

Fig. 2.18 Temperature distribution at section $y = -25$mm

2.4 Pressure distributions

Fig. 2.19 shows the static pressure distribution and Fig. 2.20 shows the total pressure distribution at the central vertical section (z = 0) of the present master joint model. As shown in these figures, the pressure difference between the inlet and the outlet of the present master joint is relatively large, so this model requires high pressure for hot water flows through the master joint. It means a pump with a higher capacity must be used to transport the flow through the present master joint.

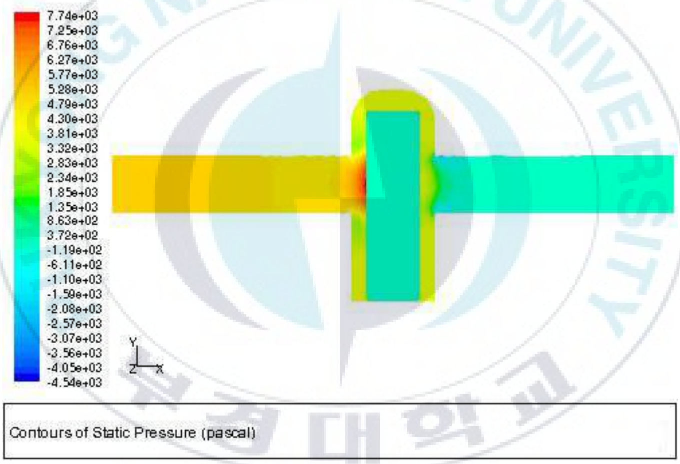

Fig. 2.19 Static pressure distribution at the central vertical section (z = 0)

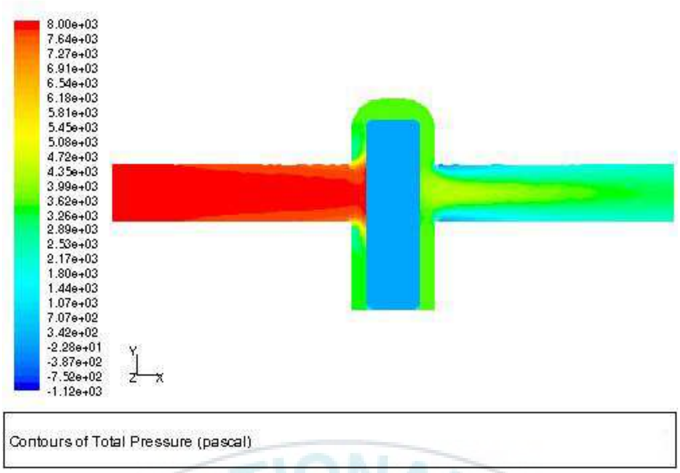

Fig. 2.20 Total pressure distribution at the central vertical section (z = 0)

CHAPTER 3

EVALUATION OF THE EFFECTS OF THE MAIN PIPE DIAMETER

3.1 Introduction to the four types of the main pipe diameter

Besides the master joint, another part also playing an important role and affecting the efficiency of the floor heating system is the main hot water pipe. The diameter of the main pipe has many influences on the heat transfer possibility of this system. Four types called type A, type B, type C and type D, which are corresponding to 13.5mm, 15.5mm, 17.5mm and 19.5mm of the main pipe diameter respectively, are discussed to see the effects of the main pipe diameter on this floor heating system. The geometry dimensions of the four types of the main pipe diameter are shown in Fig. 3.1.

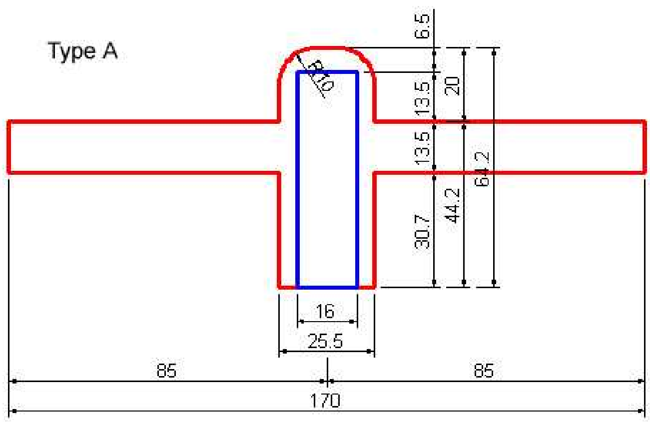

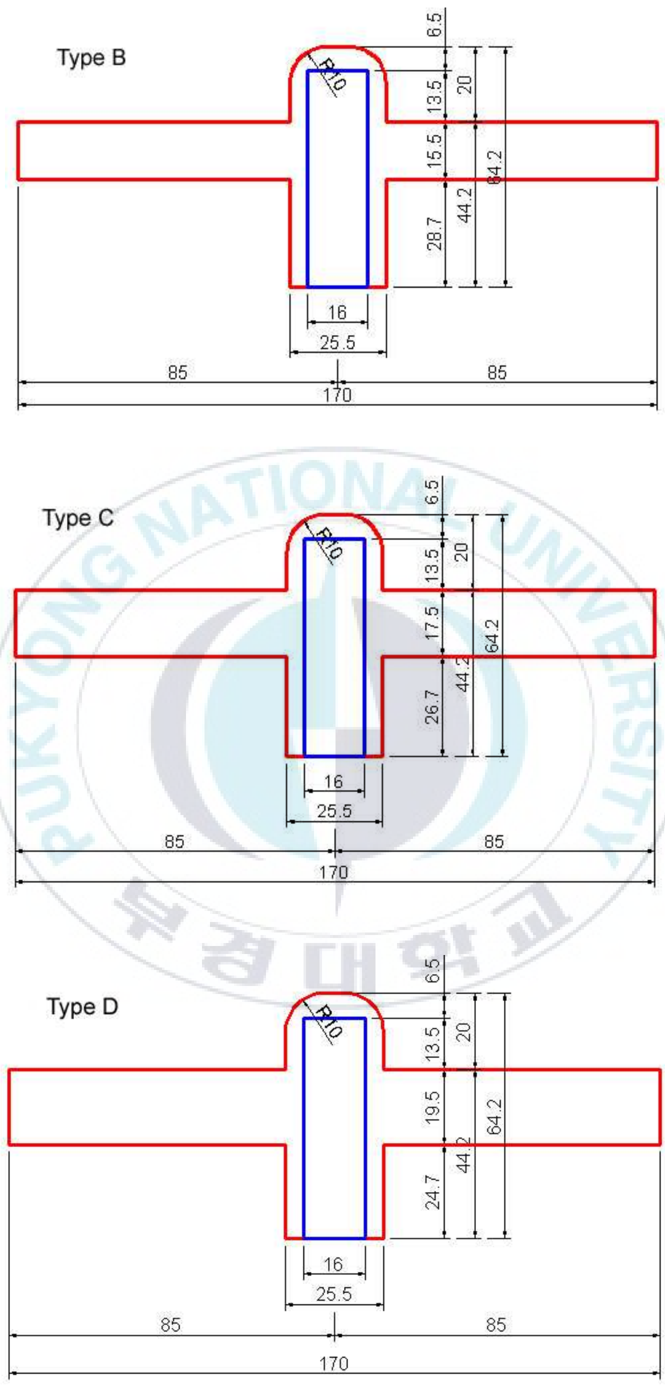

Fig. 3.1 Geometry dimensions of the type A, B, C, D models

GAMBIT was also used for creating and meshing these four models and FLUENT was used for solving the computations and distributing the results. Numerical simulations were carried out to see the flow characteristics, temperature distributions of the four models. The purpose of this chapter is to compare velocity, temperature and heat transfer of the four models in the same conditions to see the effects of the main pipe diameter on this heating system.

For these four models in this chapter, a finite volume method was used for the discretization of the continuity equation, the momentum equations, and the energy equation. Hybrid scheme was used for the convection-diffusion terms and standard k-ε model was used as a turbulent model. Tetrahedral volume meshing scheme was used for meshing these four models. The grids for the four types of the main pipe diameter models used in the numerical simulations are shown in Fig. 3.2.

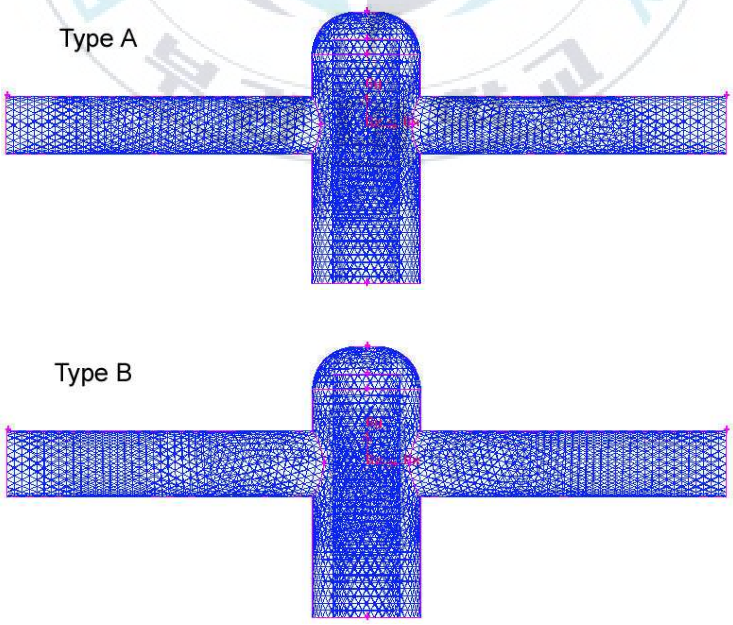

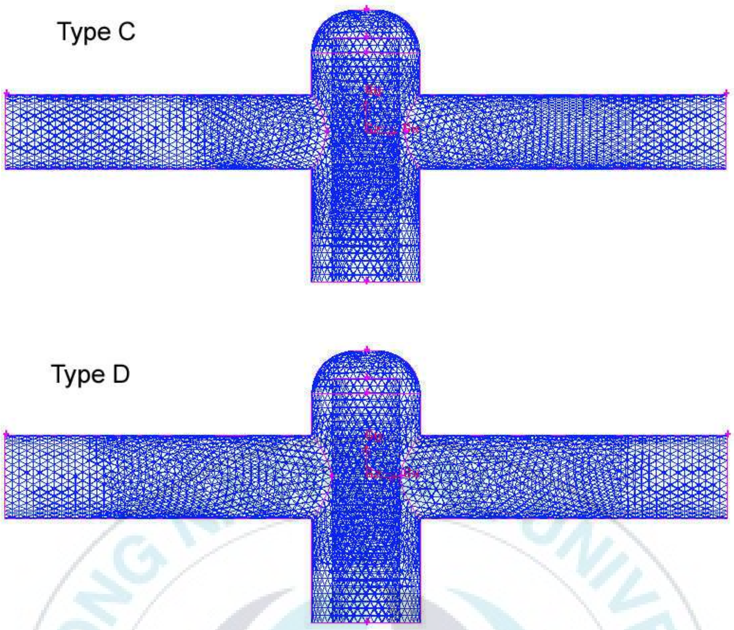

Fig. 3.2 Grids for numerical analysis of the type A, B, C, D models

In order to compare four types of the main pipe diameter, the same boundary conditions were applied to these four models. For pressure boundary conditions, pressure differences between the inlets and the outlets are about 5250 Pa. Total pressures were given at the inlets of the main pipes and static atmospheric pressures were given at the outlets of the main pipes. For temperature boundary conditions, 80^{o}C for hot water was used at the inlets of the main pipes, adiabatic conditions were used at walls of the master joints and isothermal conditions of 54^{o}C for the heat pipe or thermal siphon walls, were used in the numerical simulations.

3.2 Comparisons of the velocity vectors distributions for the four types of the main pipe diameter

To compare the effects of the main pipe diameter on this heating system, the velocity vectors distributions of the flows at the central horizontal sections (y = 0) of the four models are presented in Fig. 3.3. As shown in this figure, the velocity of the flow is directly proportional to the diameter of the main pipe. It means that the velocity increases when the diameter of the main pipe increases, for the same pressure and temperature boundary conditions.

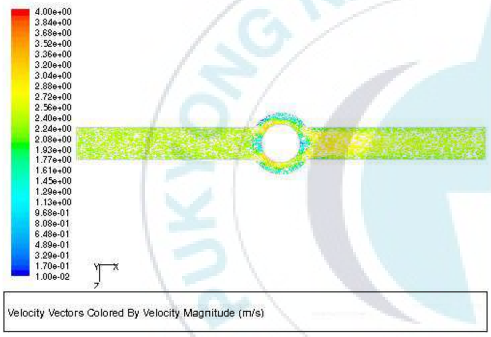

(a) Type A

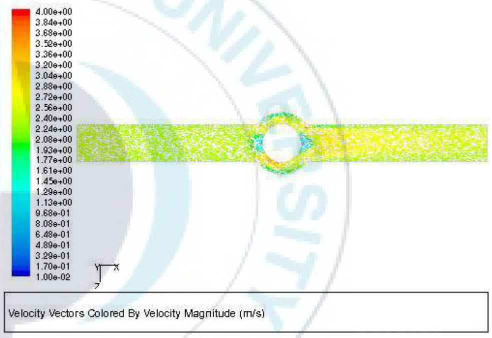

(b) Type B

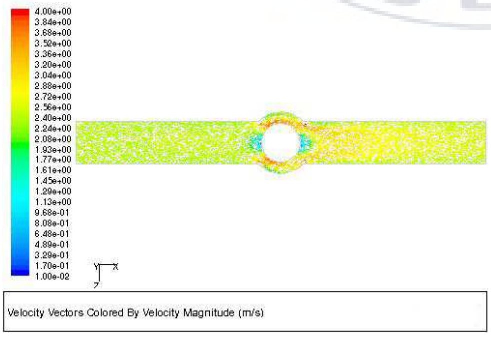

(c) Type C

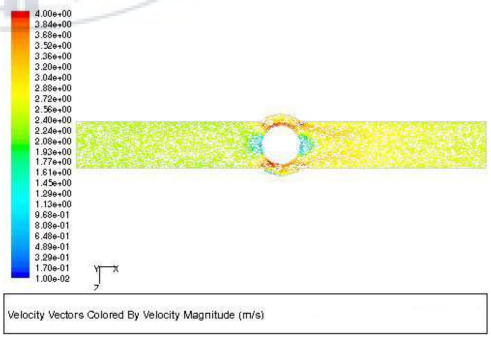

(d) Type D

Fig. 3.3 Velocity vectors distributions at the central horizontal sections for the four types of the main pipe diameter (y = 0)

Fig. 3.4 shows in more detail velocity vectors around the heat pipe or thermal siphon at the central horizontal sections (y = 0) of these four models. As shown in Fig. 3.4, the velocities around the heat pipe or thermal siphon are very large due to the small passing area. Separated flows are also observed in all four models, but the velocity of type D is larger than the velocities of other types. It means that the flow rate of type D is largest, so the heat transfer can be enhanced to the heat pipe or thermal siphon.

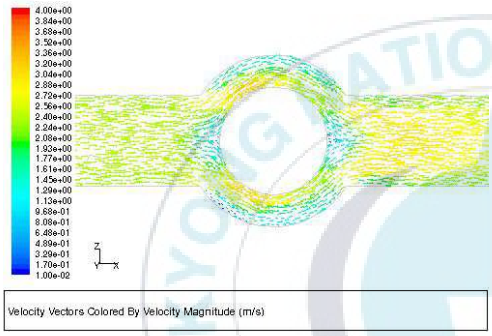

(a) Type A

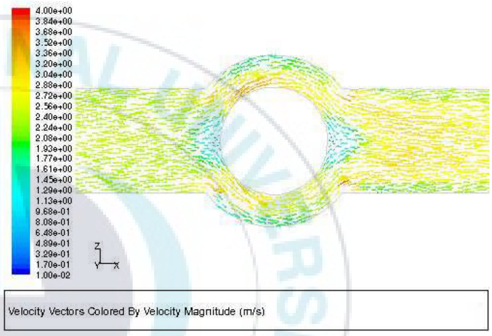

(b) Type B

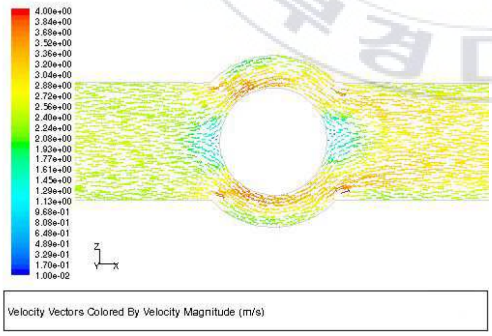

(c) Type C

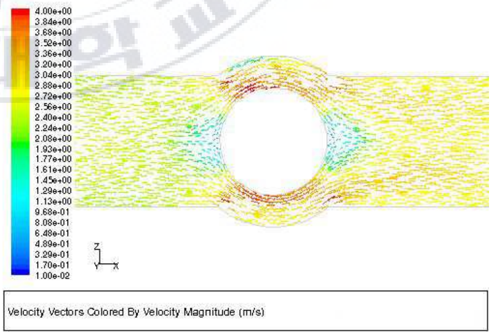

(d) Type D

Fig. 3.4 Velocity vectors distributions around the thermal siphons at the central horizontal sections for the four types of the main pipe diameter (y = 0)

Fig. 3.5 shows the velocity vectors distributions at the central vertical sections (z = 0) of the four models, for the same boundary conditions. As also shown in this figure, separated flows happened similarly at the upstream and downstream main pipes in all four models, but the velocities of the four models are not the same. The velocity of type D is largest among these four models. Therefore the heat transferred to the heat pipe or thermal siphon of type D is more than the heat transferred to other types.

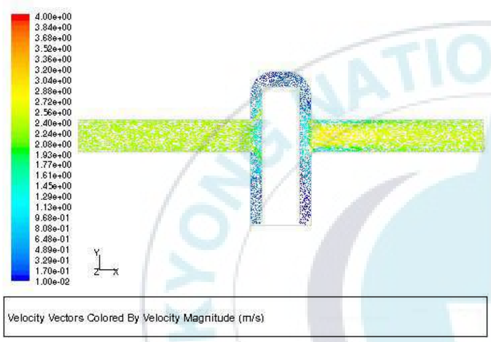

(a) Type A

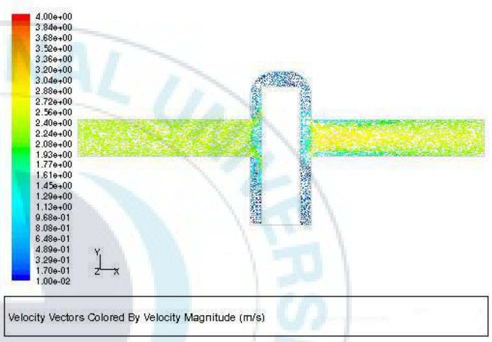

(b) Type B

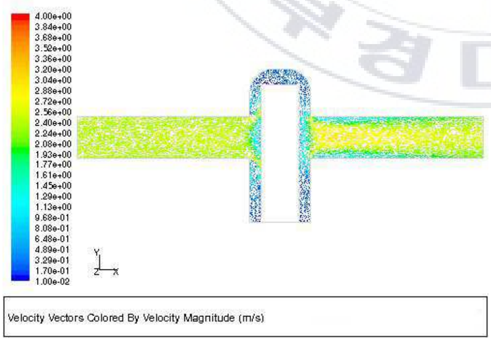

(c) Type C

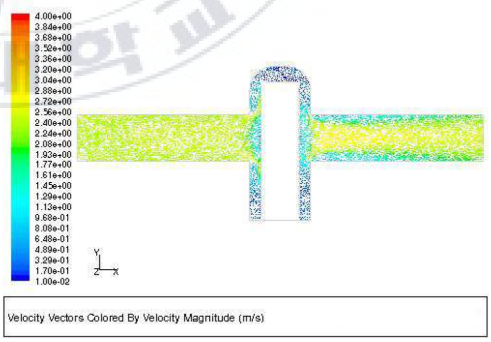

(d) Type D

Fig. 3.5 Velocity vectors distributions at the central vertical sections for the four types of the main pipe diameter (z = 0)

The comparisons of velocities around the heat pipe or thermal siphon are shown in more detail at the central vertical sections (z = 0) of the four models in Fig. 3.6. As shown in this figure, the velocity of the big main pipe diameter is larger than the velocity of the small main pipe diameter. Hence the heat transferred to the heat pipe or thermal siphon of the big main pipe diameter model is more than the heat transferred to the small main pipe diameter model.

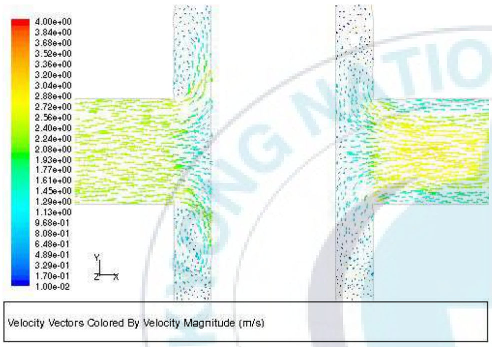

(a) Type A

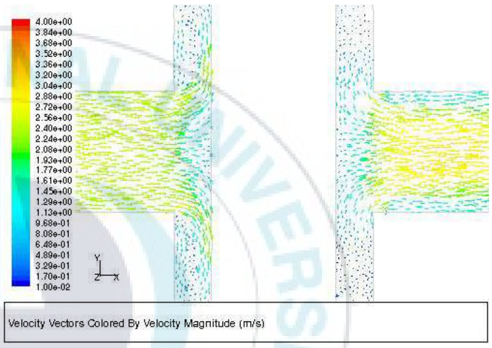

(b) Type B

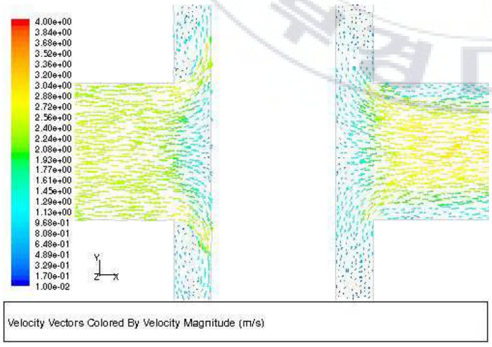

(c) Type C

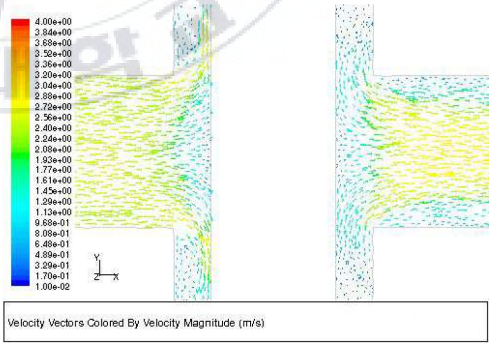

(d) Type D

Fig. 3.6 Velocity vectors distributions around the thermal siphons at the central vertical sections for the four types of the main pipe diameter (z = 0)

3.3 Comparisons of the temperature fields for the four types of the main pipe diameter

Fig. 3.7 shows the temperature distributions at the central horizontal sections (y = 0) of the four models, for the same boundary conditions. As shown in this figure, the temperature drop after the heat pipe or thermal siphon is relatively large for type A and relatively small for type D. For type D, the temperature is nearly uniform around the heat pipe or thermal siphon.

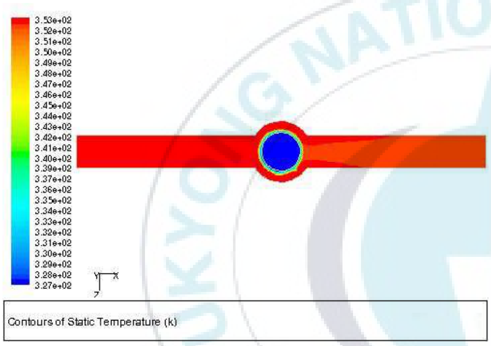

(a) Type A

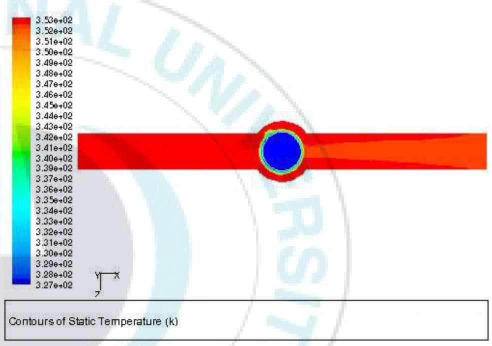

(b) Type B

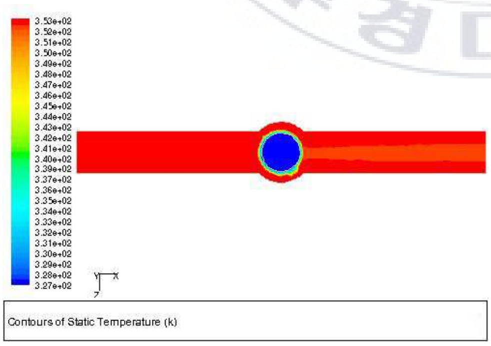

(c) Type C

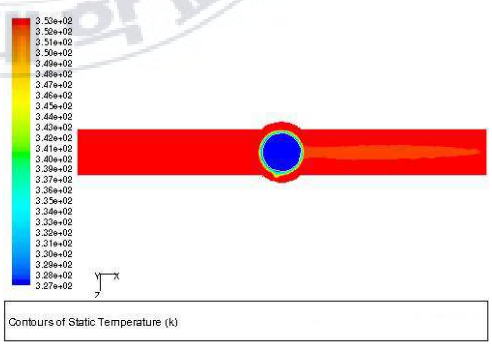

(d) Type D

Fig. 3.7 Temperature distributions at the central horizontal sections for the four types of the main pipe diameter (y = 0)

Fig. 3.8 shows the temperature distributions of the four models at the central vertical sections (z = 0), for the same boundary conditions. For type A, the temperature difference of before and after the master joint is relatively large. The heat transfer mostly happens at the front side of the heat pipe or thermal siphon. Conversely, the temperatures before and after the master joint of type D are nearly equal so the heat transfer can be enhanced to the heat pipe or thermal siphon.

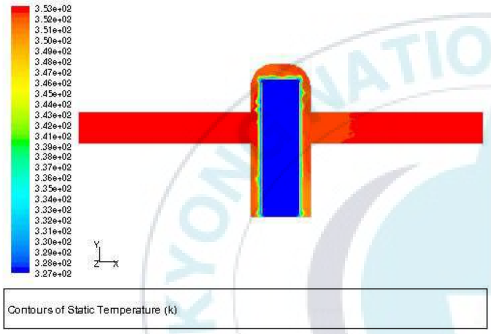

(a) Type A

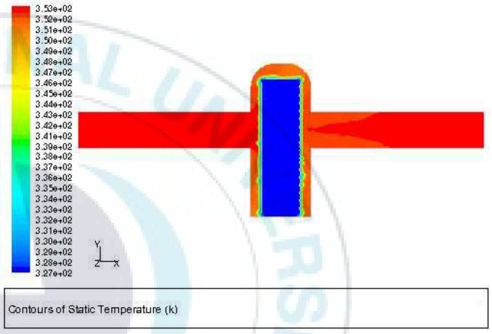

(b) Type B

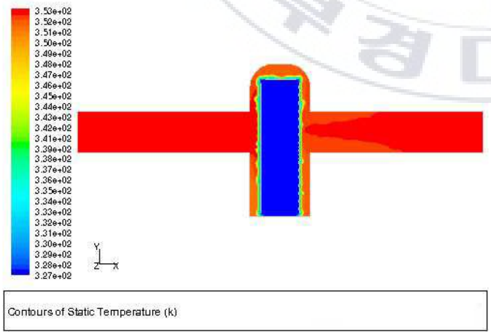

(c) Type C

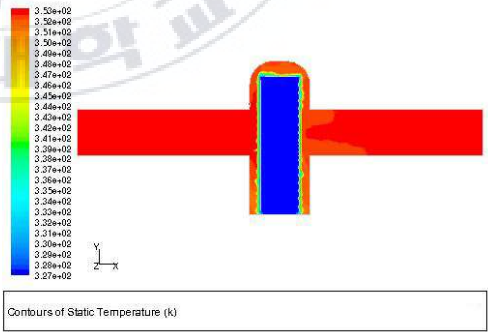

(d) Type D

Fig. 3.8 Temperature distributions at the central vertical sections for the four types of the main pipe diameter (z = 0)

Fig. 3.9 shows in more detail the temperature distributions around the heat pipe or thermal siphon at the central vertical sections (z = 0) of the four models. As shown in this figure, the heat pipe or thermal siphon of the big main pipe diameter model can contract a greater temperature than the heat pipe or thermal siphon can of the small main pipe diameter model. Therefore the amount of heat transferred from the hot water to the heat pipe or thermal siphon of the big main pipe diameter model, is larger than in the small main pipe diameter model.

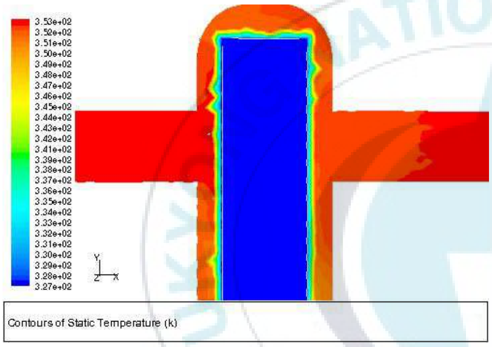

(a) Type A

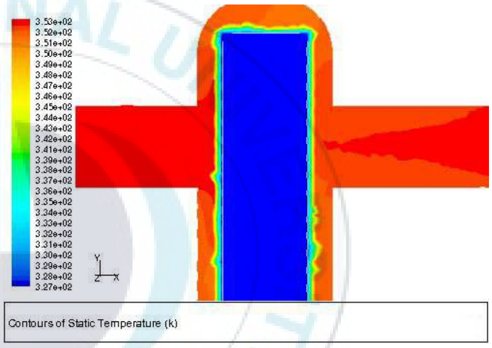

(b) Type B

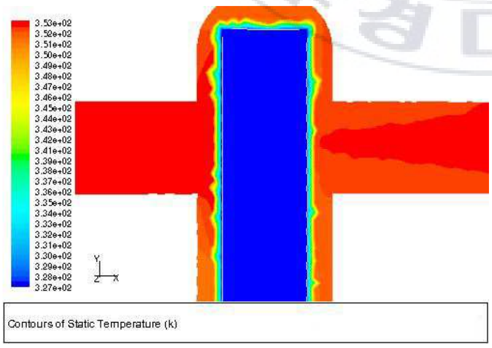

(c) Type C

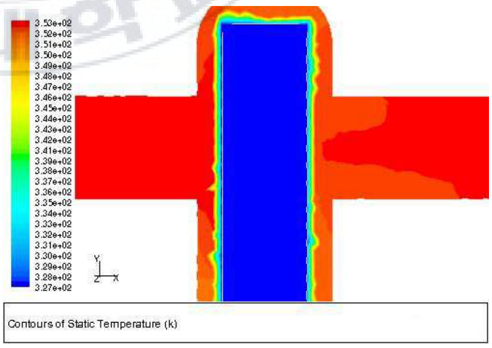

(d) Type D

Fig. 3.9 Temperature distributions around the thermal siphons at the central vertical sections for the four types of the main pipe diameter (z = 0)

3.4 Comparisons of heat transfer for the four types of the main pipe diameter

From Table 3.1 to Table 3.4 below, the results calculated in the simulations for four types of the main pipe diameter are summarized. In these four tables, the pressure differences Δp (Pa) between the inlets and the outlets, the mass flow rates $\dot{m}$ (kg/s), the flow rates Q (m^3/s) and the heat transfer rates $\dot{Q}$ (J/s) of the flows passing through four models, are presented. As clearly shown in these tables, the big main pipe diameter model is more effective than the small main pipe diameter model for cases with the same pressure difference Δp.

Table 3.1 Results of the type A (d = 13.5mm)

Type A (d = 13.5mm)				
Δp (Pa)	Mass flow rate $\dot{m}$ (kg/s)	Flow rate Q (m^3/s)	Heat transfer rate $\dot{Q}$ (J/s)	$\Delta p \times Q$ (W)
1349.854	0.16122	0.0001615	323.24835	0.21802
2684.832	0.22930	0.0002297	433.08352	0.61674
4015.715	0.28165	0.0002822	517.80740	1.13308
5344.146	0.32585	0.0003264	588.94622	1.74453
6670.854	0.36482	0.0003655	651.37664	2.43806

Table 3.2 Results of the type B (d = 15.5mm)

Type B (d = 15.5mm)				
Δp (Pa)	Mass flow rate $\dot{m}$ (kg/s)	Flow rate Q (m^3/s)	Heat transfer rate $\dot{Q}$ (J/s)	$\Delta p \times Q$ (W)
1330.017	0.21618	0.0002166	378.32141	0.28805
2645.829	0.30734	0.0003079	512.97492	0.81464
3957.717	0.37743	0.0003781	616.40033	1.49645
5267.261	0.43659	0.0004374	703.55993	2.30378
6575.180	0.48875	0.0004896	780.22334	3.21944

Table 3.3 Results of the type C (d = 17.5mm)

Type C (d = 17.5mm)				
Δp (Pa)	Mass flow rate $\dot{m}$ (kg/s)	Flow rate Q (m^3/s)	Heat transfer rate $\dot{Q}$ (J/s)	$\Delta p \times Q$ (W)
1318.991	0.27829	0.0002788	421.01118	0.36773
2625.128	0.39543	0.0003961	575.07485	1.03993
3927.741	0.48548	0.0004864	693.54669	1.91029
5228.263	0.56148	0.0005625	792.93295	2.94086
6527.336	0.62848	0.0006296	879.88293	4.10972

Table 3.4 Results of the type D (d = 19.5mm)

Type D (d = 19.5mm)				
Δp (Pa)	Mass flow rate $\dot{m}$ (kg/s)	Flow rate Q (m^3/s)	Heat transfer rate $\dot{Q}$ (J/s)	$\Delta p \times Q$ (W)
1307.749	0.37616	0.0003768	482.59059	0.49280
2602.907	0.53916	0.0005401	664.36380	1.40591
3894.638	0.65812	0.0006593	795.59857	2.56777
5184.348	0.75000	0.0007514	895.78672	3.89528
6472.623	0.81803	0.0008195	968.44684	5.30432

The simulation data above is used to plot graphs for comparing the flow rate Q (m^3/s), the heat transfer rate $\dot{Q}$ (J/s) and the pump capacities needed for the four models. With these graphs, it is easily to know the effects of the main pipe diameter on the heating system.

Fig. 3.10 plots the pressure differences Δp (Pa) between the inlets and the outlets versus the flow rates Q (m^3/s) of the flows passing through the four models. This figure obviously shows the comparison of the flow rates among the four types of the main pipe diameter. The flow rate passed through the big main pipe diameter model is much more than through the smaller one, for the same given pressure difference Δp.

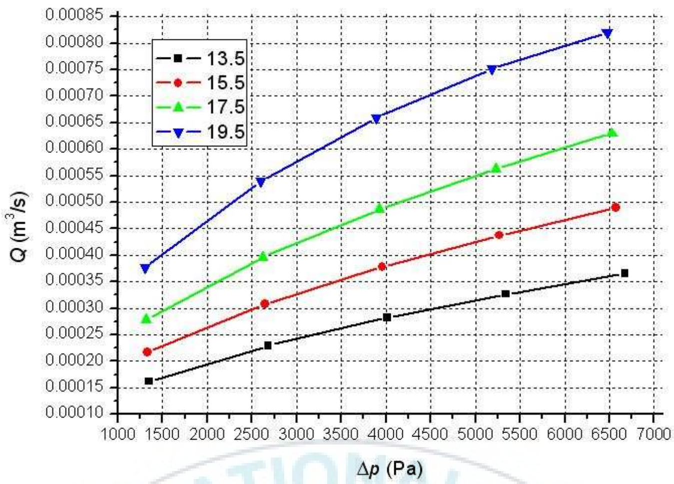

Fig. 3.10 Pressure difference Δp (Pa) vs. flow rate Q (m^3/s)

The comparison of the heat transfer rates among the four types of the main pipe diameter are plotted in Fig. 3.11. This figure shows the graph of the pressure differences Δp (Pa) between the inlets and the outlets versus the heat transfer rates $\dot{Q}$ (J/s) of the four models. For the same given pressure difference Δp, the heat transferred to the heat pipe or thermal siphon of the big main pipe diameter model, is much larger than the heat transferred to the smaller model.

Fig. 3.12 shows the relationship between the pump capacities $\Delta p \times Q$ (W) and the heat transfer rates $\dot{Q}$ (J/s) of the four types of the main pipe diameter. With the same heat transferred to the system, the big main pipe diameter model needs a smaller pump capacity than the small model.

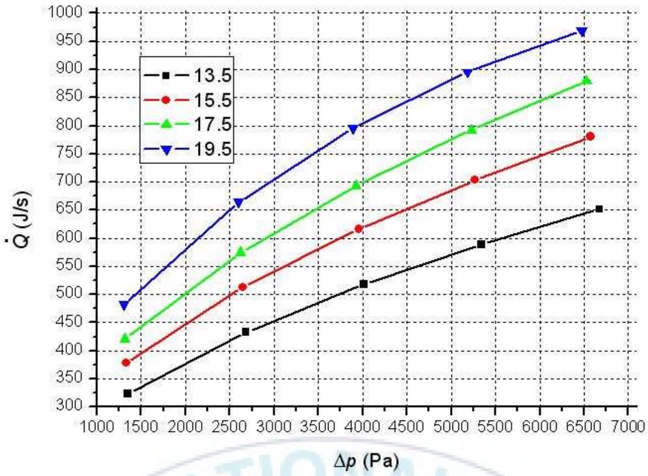

Fig. 3.11 Pressure difference Δp (Pa) vs. heat transfer rate $\dot{Q}$ (J/s)

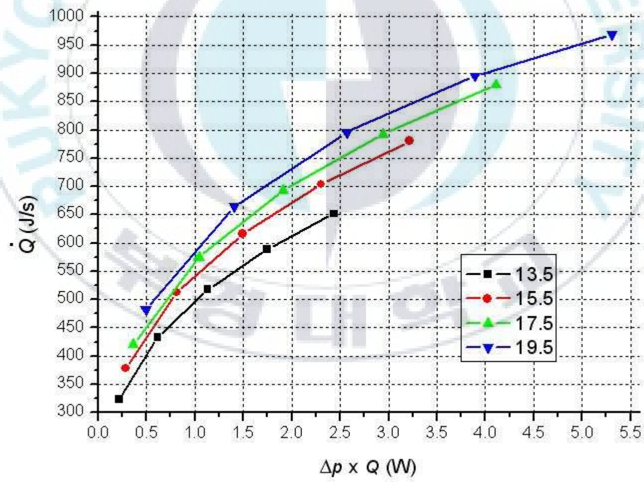

Fig. 3.12 Pump capacity P (W) vs. heat transfer rate $\dot{Q}$ (J/s)

CHAPTER 4

NEW MODEL OF MASTER JOINT; THE COMPARISONS BETWEEN THE PRESENT MODEL AND THE NEW MODEL

4.1 Introduction to the new master joint model

As already presented and discussed in chapter 2, the present master joint has some weak points. For example, the velocity and flow rate of the flow passing through the master joint are small, thermal energy of hot water transferred to heat pipe or thermal siphon is small, and pressure difference between the inlet and the outlet of the present master joint is large so the present model needs a pump with high capacity for transporting hot water.

A new master joint model is recommended to reduce these weak points mentioned above. Another weak point also has to be decreased in the new model as separated flows occurred near the heat pipe or thermal siphon. Separated flow is a cause of reducing velocity of the flow so it reduces the heat transferred to the floor. The purpose of this chapter is to compare velocity, temperature and heat transfer of the two master joint models in the same conditions to see the improvements of the new master joint.

Similar to calculating the present master joint model, GAMBIT was used for creating and meshing the new master joint model and FLUENT was used for solving the computations and distributing the results. Numerical simulations were carried out to see the flow patterns, temperature distributions and pressure distributions of this new model. A finite volume method was used for the discretization of the continuity equation, the momentum equations, and the energy equation. Hybrid scheme was used for the convection-diffusion terms and standard k-ε model was used as a turbulent model. Tetrahedral volume meshing scheme was used for meshing this new model. The grids for the new master joint model used in the numerical simulations are shown in Fig. 4.1.

Fig. 4.1 Grids for numerical analysis of the new master joint model

For comparing two master joint models, the same boundary conditions were applied to the two models. Pressure differences between the inlets and the outlets of the two models are about 5230 Pa. For temperature boundary conditions, 80^{o}C for hot water was used at the inlets of the main pipes, adiabatic conditions were used at walls of the master joints and isothermal conditions of 54^{o}C for the heat pipe or thermal siphon walls, were used in the numerical simulations.

4.2 Comparisons of the velocities passing through the master joint between the two models

Fig. 4.2 and Fig. 4.3 show velocity vectors at the central vertical sections (z = 0) and at the central horizontal sections (y = 0), respectively of the two master joint models. As shown in these figures, especially in Fig. 4.2, for the present master joint model, velocities at the upper and lower parts are very small, while velocities only at the center part are relatively large. Also clearly shown in these figures, velocities for the new model are generally larger than those for the present model. Although separated flows are also observed for the new model, velocities are very large over a wide area of the new master joint. It means that the flow rate of the new model is generally larger than the flow rate of the present model, so the heat transfer can be enhanced to the heat pipe or thermal siphon.

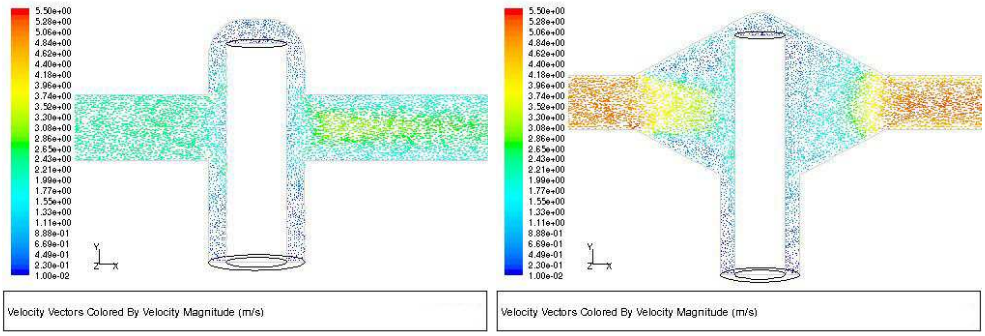

(a) (b)

Fig. 4.2a Velocity vectors distribution at the central vertical section of the present master joint model (z = 0)

Fig. 4.2b Velocity vectors distribution at the central vertical section of the new master joint model (z = 0)

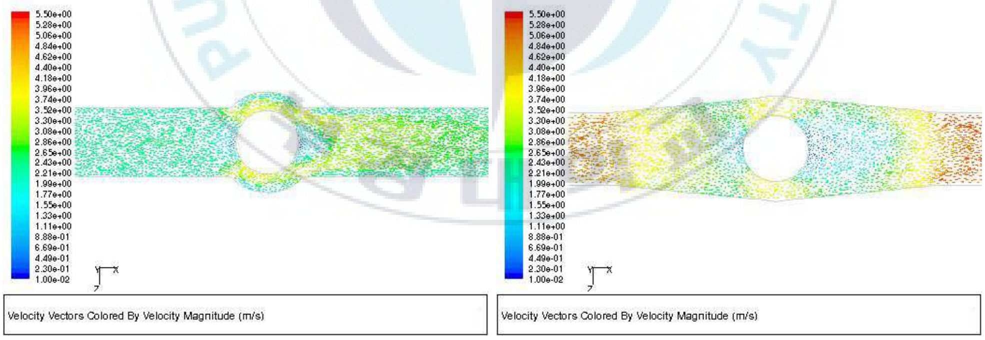

(a) (b)

Fig. 4.3a Velocity vectors distribution at the central horizontal section of the present master joint model (y = 0)

Fig. 4.3b Velocity vectors distribution at the central horizontal section of the new master joint model (y = 0)

From Fig. 4.4 to Fig. 4.14, velocity vectors in some horizontal sections with 5mm intervals on the *y* axis are shown. The left side figures show velocity vectors of the present model while the right side figures show the velocity vectors of the new model at the same sections. Corresponding to the color scale on the left side of these figures, velocities of the flow at all sections of the new model are larger than velocities of the flow of the present model at the same locations.

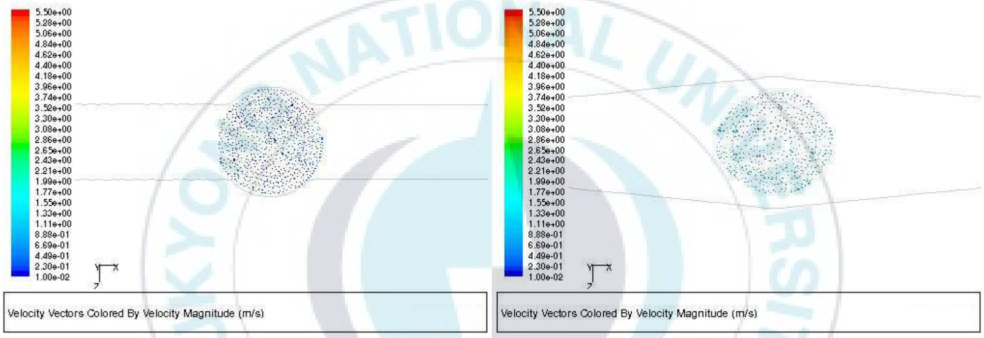

Fig. 4.4 Velocity vectors distributions at section *y* = 25mm

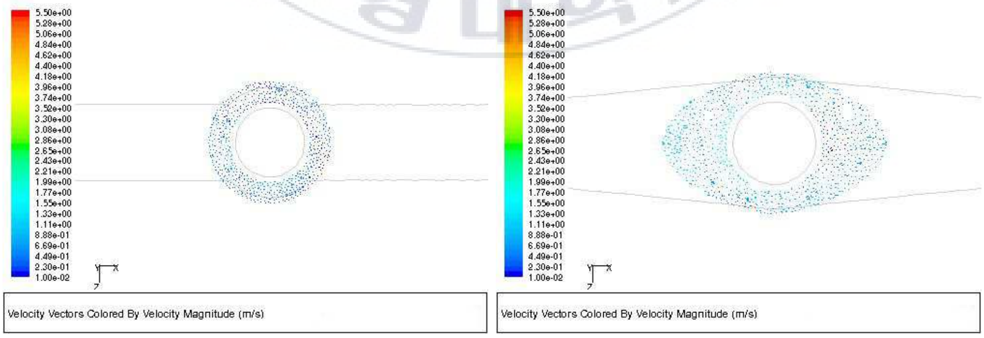

Fig. 4.5 Velocity vectors distributions at section *y* = 20mm

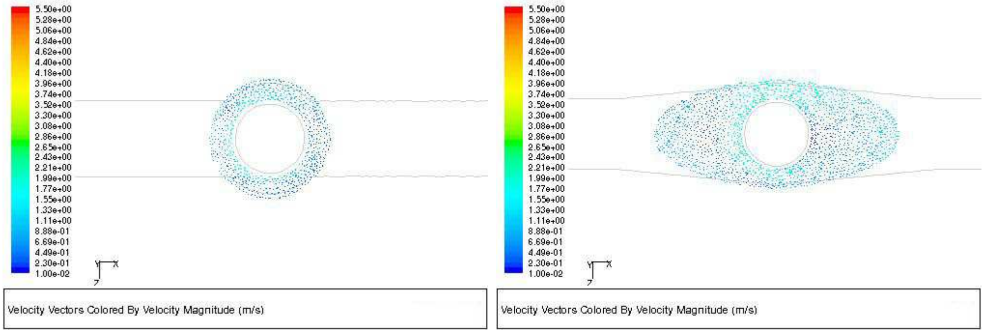

Fig. 4.6 Velocity vectors distributions at section y = 15mm

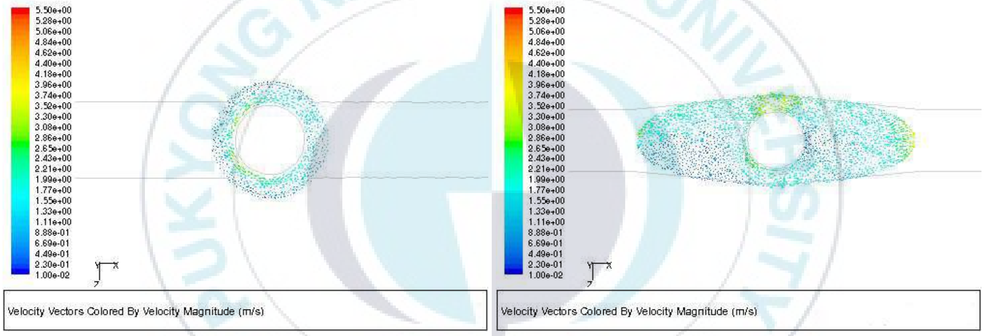

Fig. 4.7 Velocity vectors distributions at section y = 10mm

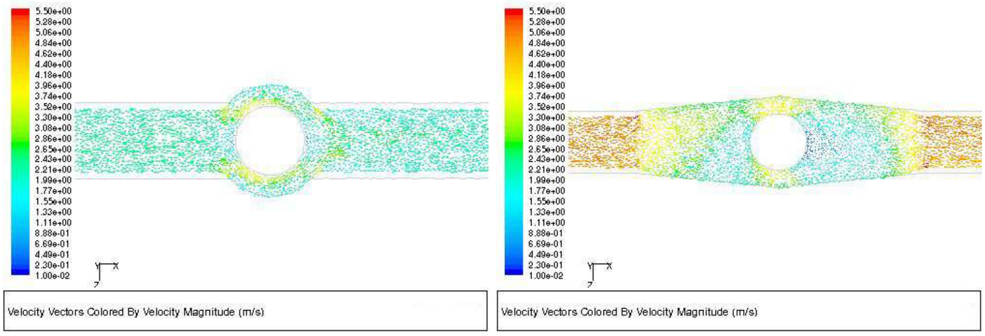

Fig. 4.8 Velocity vectors distributions at section y = 5mm

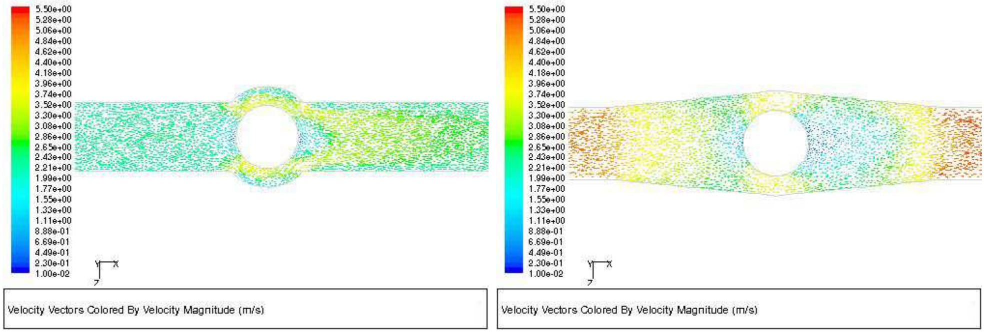

Fig. 4.9 Velocity vectors distributions at section $y = 0$

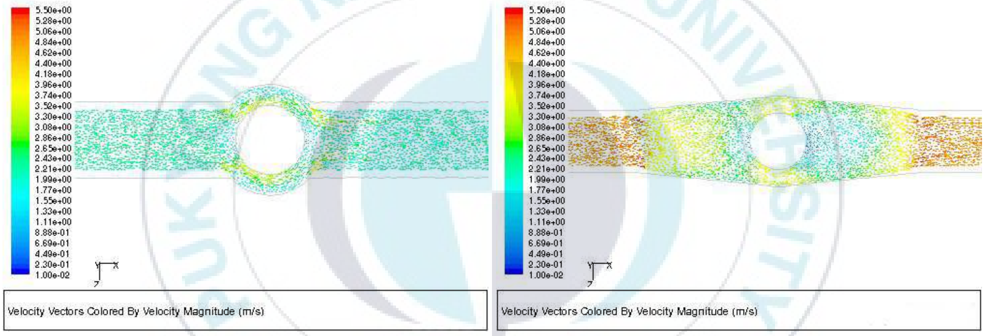

Fig. 4.10 Velocity vectors distributions at section $y = -5$mm

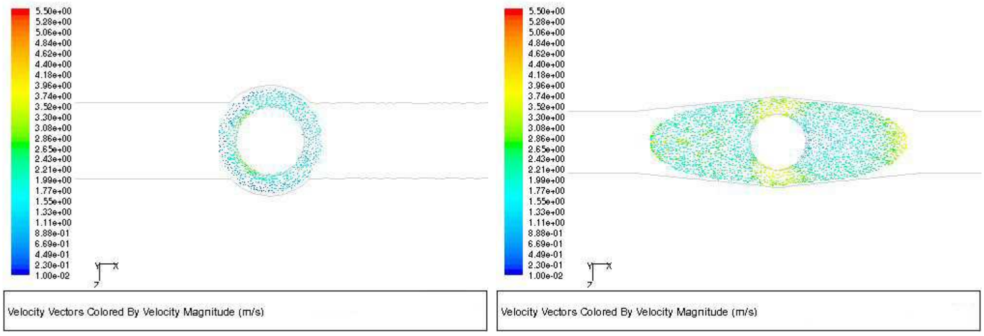

Fig. 4.11 Velocity vectors distributions at section $y = -10$mm

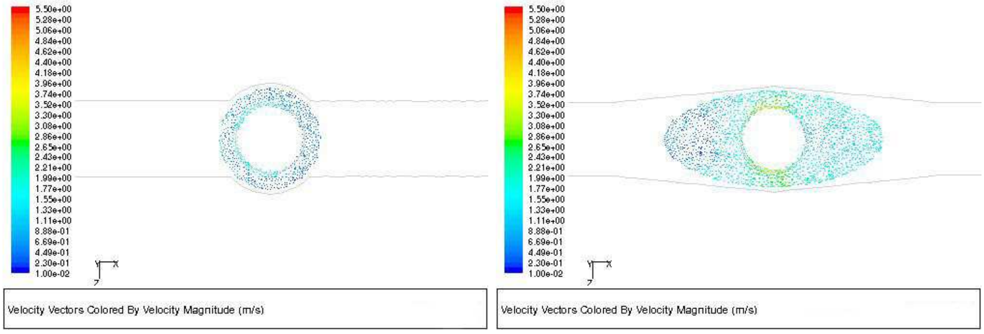

Fig. 4.12 Velocity vectors distributions at section $y = -15$mm

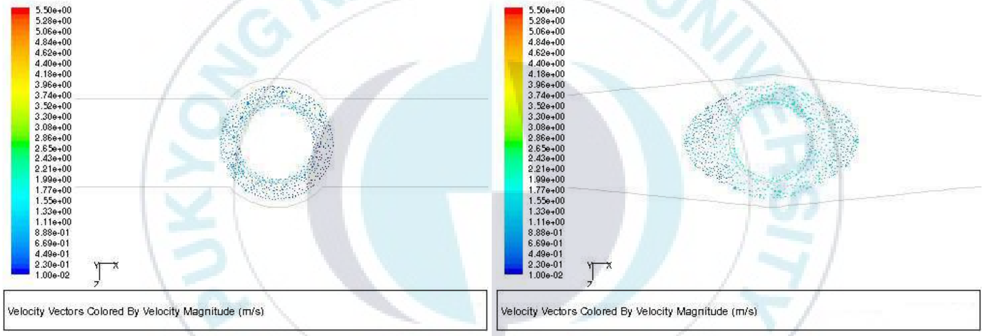

Fig. 4.13 Velocity vectors distributions at section $y = -20$mm

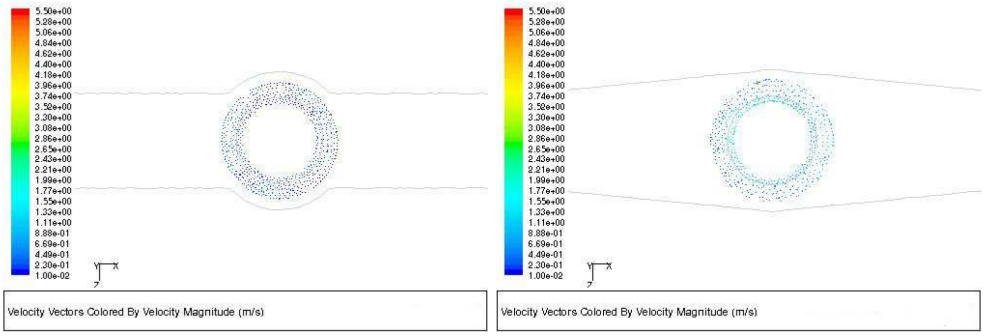

Fig. 4.14 Velocity vectors distributions at section $y = -25$mm

4.3 Comparisons of the temperature fields between the two models

Fig. 4.15 shows the temperature distributions at the central vertical section (z = 0) of the present and the new master joint model. As shown in this figure, the heat pipe or thermal siphon of the new model can contract a greater temperature than the heat pipe or thermal siphon can in the present model. Hence the amount of heat transferred from the hot water to the heat pipe or thermal siphon for the new master joint model is increased remarkably.

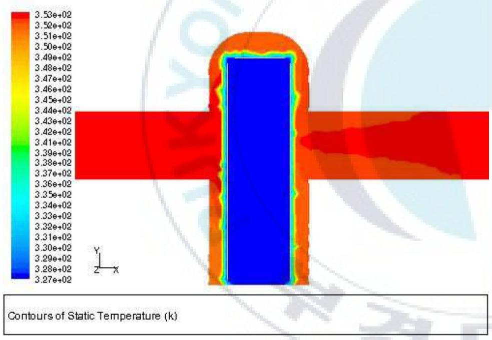

(a)

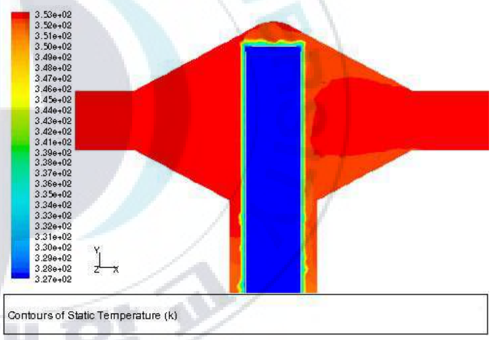

(b)

Fig. 4.15a Temperature distribution at the central vertical section of the present master joint model (z = 0)

Fig. 4.15b Temperature distribution at the central vertical section of the new master joint model (z = 0)

From Fig. 4.16 to Fig. 4.26, temperature distributions in some horizontal sections with 5mm intervals on the *y* axis are shown. The left side figures show temperature distributions of the present model while the right side figures show the temperature distributions of the new model at the same sections. Corresponding to the color scale on the left side of these figures, temperature distributions at all sections of the new model are larger than temperature distributions of the present model at the same locations.

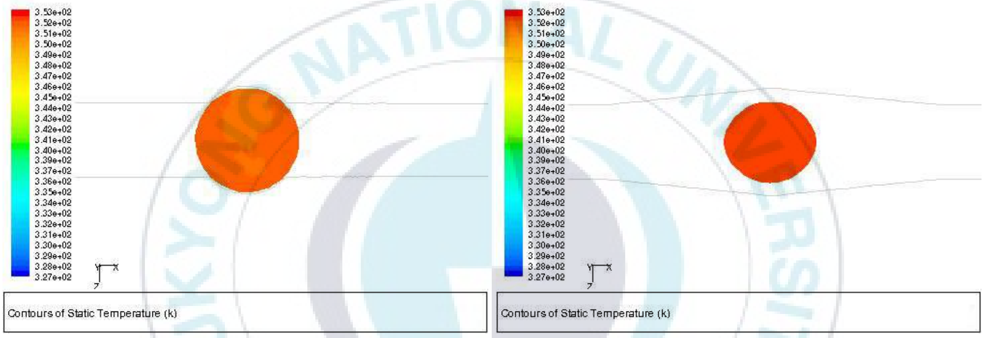

Fig. 4.16 Temperature distributions at section y = 25mm

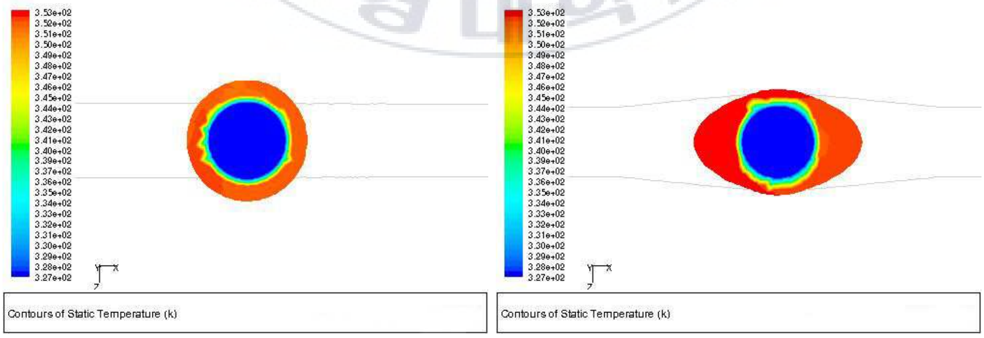

Fig. 4.17 Temperature distributions at section y = 20mm

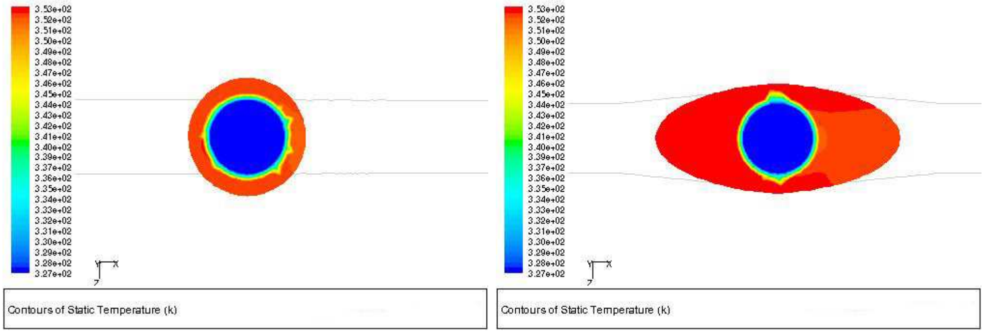

Fig. 4.18 Temperature distributions at section y = 15mm

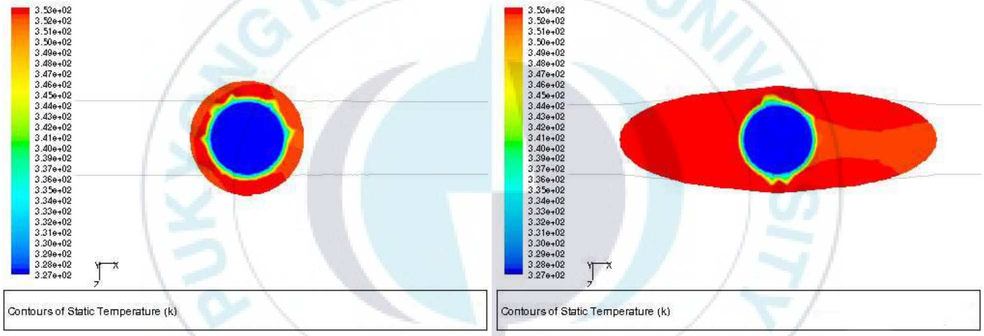

Fig. 4.19 Temperature distributions at section y = 10mm

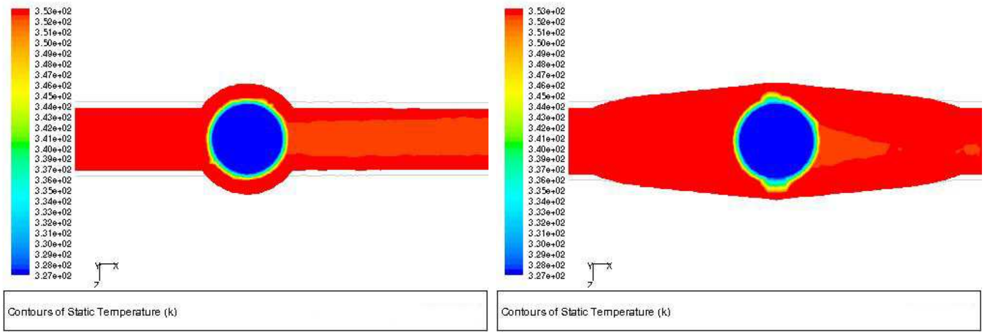

Fig. 4.20 Temperature distributions at section y = 5mm

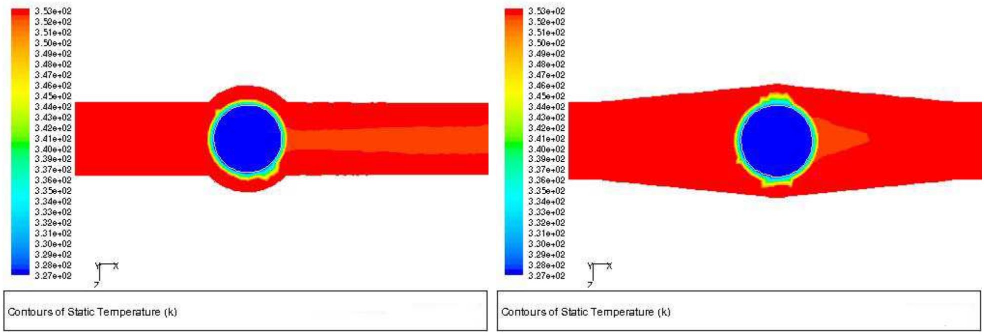

Fig. 4.21 Temperature distributions at section $y = 0$

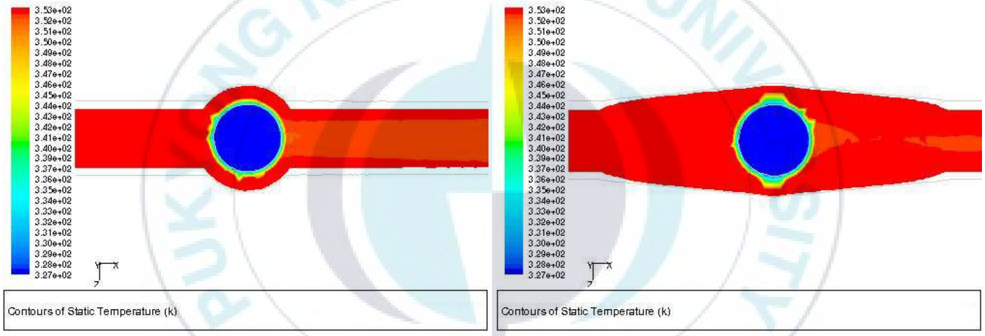

Fig. 4.22 Temperature distributions at section $y = -5$mm

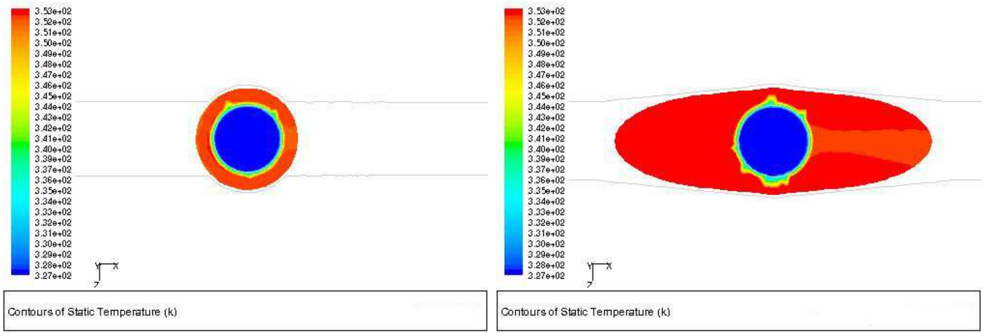

Fig. 4.23 Temperature distributions at section $y = -10$mm

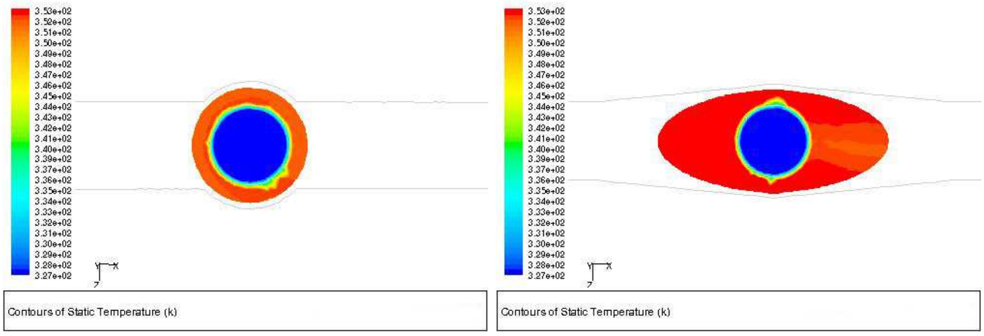

Fig. 4.24 Temperature distributions at section y = –15mm

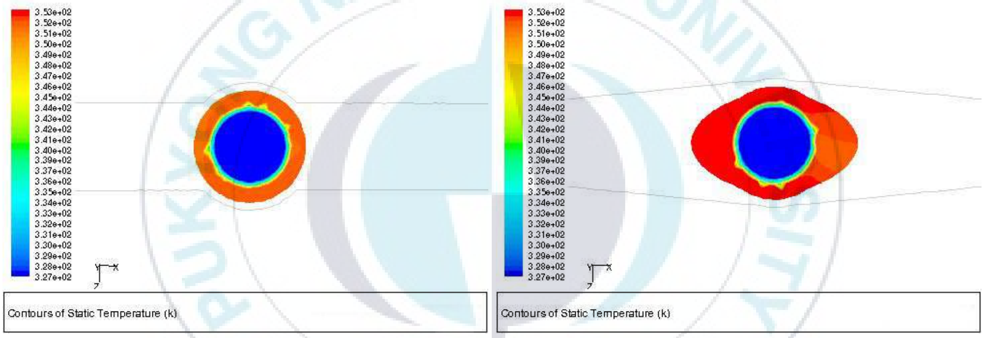

Fig. 4.25 Temperature distributions at section y = –20mm

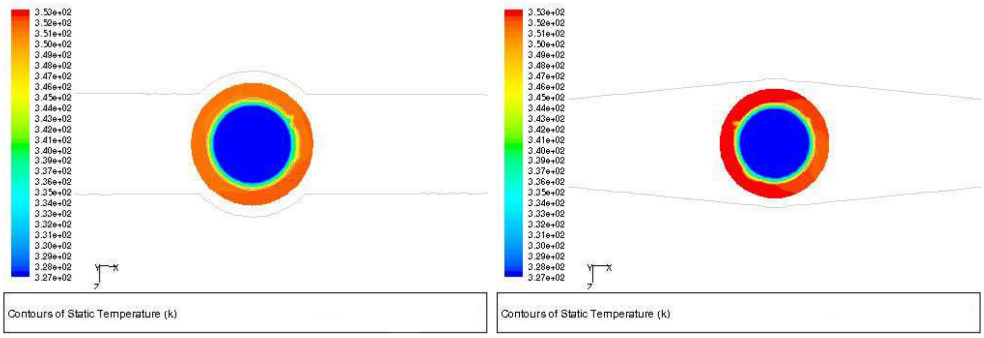

Fig. 4.26 Temperature distributions at section y = –25mm

4.4 Comparisons of heat transfer between the two models

Table 4.1 and Table 4.2 below summarize the results calculated in the simulations of the two master joint models. In these two tables, the pressure differences Δp (Pa) between the inlets and the outlets of two models, the mass flow rates $\dot{m}$ (kg/s), the flow rates Q (m^3/s) and the heat transfer rates $\dot{Q}$ (J/s) of the flows passing through two models are presented. As obviously shown in these tables, the new master joint is more effective than the present one for cases with the same pressure difference Δp.

The capacity of the pump used to supply hot water to the heating system is $P = \rho \times g \times H \times Q$, where $\rho \times g \times H$ is the pressure difference of before and behind of the pump. The thermal energy of the hot water transferred to the heat pipe or thermal siphon can be determined from:

$$\dot{Q} = \dot{m} \times C_p \times \Delta T$$

where ⁎ $\dot{m}$ is the mass flow rate (kg/s).

⁎ C_p is the constant pressure specific heat (J/kg·K). C_p = 4182 J/kg·K for water.

⁎ ΔT is the temperature difference between the inlet and the outlet of the master joint model (K).

⁎ ρ is the density of water (kg/m^3), ρ = 998.2 kg/m^3.

⁎ g is the gravitational acceleration (m/s^2), g = 9.81 m/s^2.

⁎ H is the actual head rise (m), gained by fluid flowing through a pump.

Table 4.1 Results of the present master joint model

Present master joint model				
Δp (Pa)	Mass flow rate $\dot{m}$ (kg/s)	Flow rate Q (m^3/s)	Heat transfer rate $\dot{Q}$ (J/s)	$\Delta p \times Q$ (W)
1318.991	0.27829	0.0002788	421.011	0.36773
2625.128	0.39543	0.0003961	575.075	1.03993
3927.741	0.48548	0.0004864	693.547	1.91029
5228.263	0.56148	0.0005625	792.933	2.94086
6527.336	0.62848	0.0006296	879.883	4.10972

Table 4.2 Results of the new master joint model

New master joint model				
Δp (Pa)	Mass flow rate $\dot{m}$ (kg/s)	Flow rate Q (m^3/s)	Heat transfer rate $\dot{Q}$ (J/s)	$\Delta p \times Q$ (W)
1323.168	0.57783	0.0005789	569.13	0.76594
2628.83	0.82877	0.0008303	784.614	2.18262
3929.8	1.02277	0.0010246	948.392	4.02654
5233.723	1.1877	0.0011898	1087.023	6.22732
6536.218	1.33243	0.0013348	1208.449	8.72476

The pressure differences Δp (Pa) between the inlets and the outlets versus the flow rates Q (m^3/s) of the two master joints are plotted in Fig. 4.27. This figure clearly shows the comparison of flow rates between the present and the new master joint model. For the same given pressure difference Δp, the flow rate passed through the new model is much more than through the present one.

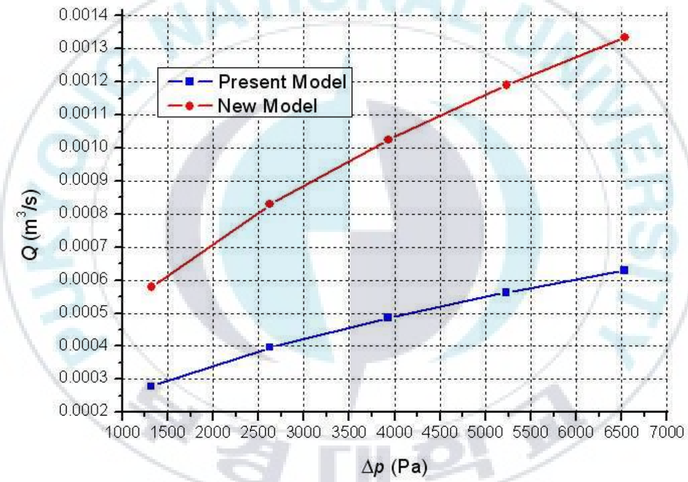

Fig. 4.27 Pressure difference Δp (Pa) vs. flow rate Q (m^3/s)

Fig. 4.28 plots the graph of the pressure differences Δp (Pa) between the inlet and the outlet versus the heat transfer rates $\dot{Q}$ (J/s) of the two models. This figure shows the comparison of heat transfer rates between the present and the new master joint model. As shown in this figure, the heat transferred to the heat pipe or thermal siphon of the new model is much larger than the heat transferred to the present model, for the same given pressure difference Δp.

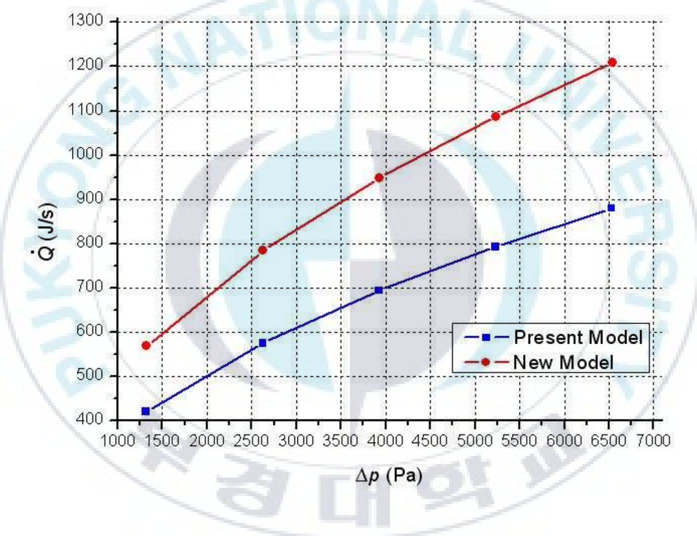

Fig. 4.28 Pressure difference Δp (Pa) vs. heat transfer rate $\dot{Q}$ (J/s)

Fig. 4.29 shows the relationship between the capacities of the pump $\Delta p \times Q$ (W) and the heat transfer rates $\dot{Q}$ (J/s) of the two models. This figure shows the comparison of the pump capacities between the present and the new master joint model and presents the efficiency of the new model beside the present one. With the same pump power, the new heating system will receive much thermal energy than the present heating system. The pressure difference between the inlet and the outlet of the present model is relatively large, compared with the new model. It means that the present model requires much higher pressure than the new model to get the same flow rate, so it is difficult to obtain a high capacity of the pump in the present model.

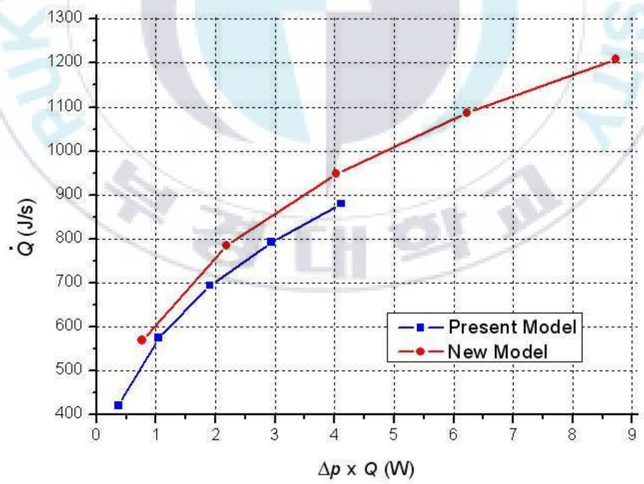

Fig. 4.29 Pump capacity P (W) vs. heat transfer rate $\dot{Q}$ (J/s)

CHAPTER 5

CONCLUSIONS

In order to increase the heat transferred to the floor, a new master joint model using heat pipe or thermal siphon was recommended in this study. This new master joint model was compared with the present one with regards to the velocity, temperature and heat transfer in the same conditions to see the improvements of the new master joint. Also in this study, four types of the main pipe diameter were presented and discussed to see the effects of the main pipe diameter on this floor heating system.

The following conclusions were obtained from the results of this study on the velocity vectors distributions, temperature fields, pressure characteristics and heat transfer for the present master joint model, four types of the main pipe diameter and the new master joint model.

- The velocity of the present master joint model is rather small. Separated flows occurred near the heat pipe or thermal siphon and prevented the flow passing through the master joint so the velocity of the flow was reduced. Temperature of the flow going out the master joint toward the outlet reduced remarkably so the amount of heat transferred from hot water to the heat pipe or thermal siphon is small. The pressure difference between the inlet and the outlet of the present master joint is relatively large, so it needs a high capacity pump to transport the flow through the present master joint.

- For the same boundary conditions, the flow patterns, velocity vectors distributions, temperature fields and heat transfer for the four types of the main pipe diameter were shown and compared to see the effects of the main pipe diameter. Velocity of the flow is directly proportional to the diameter of the main pipe. It means the velocity of type D is larger than the velocities of other types. For type D, the temperature is nearly uniform around the heat pipe or thermal siphon. The heat pipe or thermal siphon of the big main pipe diameter model can contract a greater temperature than the heat pipe or thermal siphon can of the small main pipe diameter model. Therefore the amount of heat transferred from the hot water to the heat pipe or thermal siphon of the big main pipe diameter model is larger than in the small main pipe diameter model. So the big main pipe diameter model is more effective than the small main pipe diameter model.

- The present master joint has some weak points. So it is necessary to find a new master joint to reduce these weak points. Although separated flows are also observed for the new model, velocities are very large over a wide area of the new master joint. Velocities for the new model are generally larger than those for the present model. It means that the flow rate of the new model is generally larger than the flow rate of the present model. The heat pipe or thermal siphon of the new model can contract a greater temperature than the heat pipe or thermal siphon can in the present model. So the heat transfer can be enhanced to the heat pipe or thermal siphon. With these advantages mentioned above, the new master joint is more effective than the present one.

LIST OF REFERENCES

1. Ahn, B. W., Shin, Y. T., Sohn, J. Y., July 28-31, 1996, “The optimum thickness of the thermal storage layer and the heating conditions in the ondol heating system”, International Ondol Conference, Seoul, Korea, pp. 273-280.

2. Cengel, Y. A., 1996, “Heat transfer: Introduction to thermodynamics and heat transfer”, Vol. II, McGraw-Hill, p. 840.

3. Cengel, Y. A., 1998, “Heat transfer: A practical approach”, McGraw-Hill, p. 1006.

4. Chi, S. W., 1976, “Heat pipe theory and practice”, Hemisphere Publishing Corporation, pp. 127-176.

5. Choi, Y. D., Yoon, J. H., Hong, J. K., Lee, N. H., and Kang, D. H., 1994, “Simulation of the Thermo Performance on an Ondol House with Hot water Heating in consideration of Radiation Heat Transfer”, Journal of Air-Conditioning and Refrigeration, Vol. 2, No. 1, pp. 3-16.

6. Chung, K. S., and Croome, D. J., July 28-31, 1996, “Experimental and numerical study on the thermal behaviour of hydronic ondol heating systems”, International Ondol Conference, Seoul, Korea, pp. 370-377.

7. Ferziger, J. H., Peric, M., 2002, “Computational methods for fluid dynamics”, 3rd edition, Springer, Berlin, p. 423.

8. Kim, Y. D., Min, M. K., Lee, S. H., July 28-31, 1996, “Numerical analysis on the thermal performance of three dimensional ondol floor

heating model", International Ondol Conference, Seoul, Korea, pp. 454-462.

9. Park, S. D., July 28-31, 1996, "A review on Ondol heating system and the thermal performance", International Ondol Conference, Seoul, Korea, pp. 20-40.

10. Patankar, S. V., 1980, "Numerical Heat Transfer and Fluid Flow", Hemisphere Publishing Corporation, Taylor & Francis Group, New York, p. 197.

11. Reay, D. A., 1982, "Advances in heat pipe technology", Pergamon Press, p. 818.

12. Versteeg, H. K., and Malalasekera, W., 1995, "An introduction to computational fluid dynamics: The finite volume methods", Longman, p. 257.

13. White, F. M., 1999, "Fluid mechanics", 4th edition, McGraw-Hill, Singapore, p. 826.

14. Yeo, M. S., Yang, I. H., and Kim, K. W., 2003, "Historical changes and recent energy saving potential of residential heating in Korea", Energy and Buildings, Volume 35, Issue 7, pp. 715-727.

15. Young, D. F., Munson, B. R., and Okiishi, T. H., 2004, "A brief introduction to fluid mechanics", 3rd edition, Wiley, New York, p. 533.